

Estimating Divergences in High Dimensions

Loong Kuan Lee, Nico Piatkowski, François Petitjean, and Geoffrey I. Webb

Abstract—The problem of estimating the divergence between 2 high dimensional distributions with limited samples is an important problem in various fields such as machine learning. Although previous methods perform well with moderate dimensional data, their accuracy starts to degrade in situations with 100s of binary variables. Therefore, we propose the use of decomposable models for estimating divergences in high dimensional data. These allow us to factorize the estimated density of the high-dimensional distribution into a product of lower dimensional functions. We conduct formal and experimental analyses to explore the properties of using decomposable models in the context of divergence estimation. To this end, we show empirically that estimating the Kullback-Leibler divergence using decomposable models from a maximum likelihood estimator outperforms existing methods for divergence estimation in situations where dimensionality is high and useful decomposable models can be learnt from the available data.

Index Terms—Machine Learning, Markov Random Fields, Decomposable Models, Junction Tree Algorithms, Statistical Divergence, AB-divergence, Kullback-Leibler divergence, Hellinger Distance, Concept Drift, non-Stationary Distributions, Anomaly Detection

1 INTRODUCTION

ESTIMATING the divergence between 2 distributions from sample data, hereby referred to as the *divergence estimation* problem, is an important problem in the field of machine learning. A divergence is a functional that quantifies the degree to which 2 probability distributions differ. Versions of this divergence estimation problem crop up in various fields of machine learning, such as the in analysis and adaptation of changing distributions, also known as Concept Drift [1], [2], [3], in the detection of anomalous regions in spatio-temporal data [4], and in various tasks related to the retrieval, classification, and visualisation of time series data [5].

Due to its importance, there are numerous methods that have been developed to tackle this problem in the high dimensional setting. Specifically, for estimating the divergence between *discrete distributions*, which is the focus of this paper, most methods are general and do not make any assumptions regarding the variables and domain of these distributions. Instead they interpret the data from any discrete distribution as being from a uni-variate distribution with a support¹ size S based on the number of unique items in the sampled data. However, in the worst case, the support size of any k -variate discrete distribution grows exponentially with respect to k . Furthermore, as we will show in Section 7.2, these existing methods do not scale well past 30 binary variables. The question then is, assuming these distributions have a large support due to having a large number of variables, k , is it possible to exploit this assumption to assist in the divergence estimation problem.

Given this assumption on the distributions, we will show that we can then exploit it by using a class of probabilistic

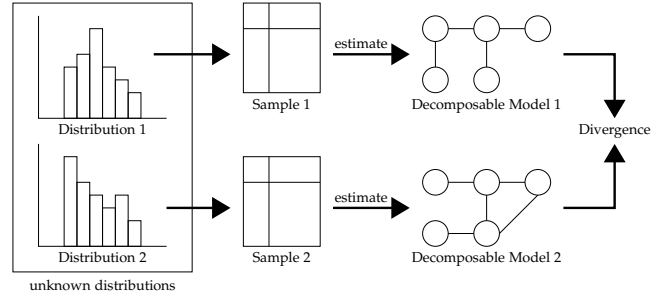


Fig. 1. Overview of proposed approach for divergence estimation. The approach first learns 2 decomposable models from samples of 2 distributions. The divergence between the distributions is estimated by computing the divergence between the decomposable models.

graphical models, called decomposable models, to essentially decompose the problem of divergence estimation into smaller sub-problems. Decomposability is a fundamental property of probabilistic graphical models. The underlying result was discovered independently by different groups in the 1970s. More precisely, it was shown in [6], [7] that the conditional independence structure \mathcal{G} of the underlying random variable X can be exploited resulting in the factorization of the joint distribution into factors with at most $\text{tw}(\mathcal{G})$ number of variables, where $\text{tw}(\mathcal{G})$, known as the *treewidth* of \mathcal{G} , is much smaller than the number of dimensions n . It is important to understand that the existence of \mathcal{G} is not an assumption. For each and every n -dimensional random variable, it is guaranteed that a graph with n vertices exists that encodes the conditional independence structure of X . In the worst-case, \mathcal{G} is fully connected, and thus $\text{tw}(\mathcal{G}) = n$. In that case, the model decomposes into a single factor. In the case that the treewidth is strictly smaller than the number of variables, \mathbb{P} will decompose into multiple factors.

As we will further discuss in Section 1.2, our proposed approach will involve first learning 2 decomposable models using samples from each target distribution, and then computing the divergence between these models. An illustration of this general approach can be found in Figure 1. Since

• L.K. Lee, F. Petitjean, and G.I. Webb are with the Department of Data Science and AI, Monash University, Melbourne, Australia.
 • N. Piatkowski is with Fraunhofer Institute for Intelligent Analysis and Information Systems IAIS, Schloss Birlinghoven, 53757 Sankt Augustin, Germany.
 • E-mail: loong.kuan.lee@gmail.com

Manuscript received

1. The support of a distribution is the subset of the domain where each item in the subset has a non-zero probability.

there are existing methods to learn decomposable models from data, the focus of this paper will be a method to compute the $\alpha\beta$ -divergence between 2 decomposable models.

1.1 Problem: Divergence Estimation

There are many different divergences, each useful for different purposes, that one might want to estimate using sample data. Some well known divergences include the Kullback-Leibler Divergence, the χ^2 divergence, and the Hellinger Distance. In this paper we focus on a class of divergences called the $\alpha\beta$ -divergence [8], which includes divergences such as the Kullback-Leibler divergence and the Hellinger Distance. Further details regarding divergences and the $\alpha\beta$ -divergence can be found in Section 2.3.

However, instead of directly focusing on the problem of estimating the $\alpha\beta$ -divergence, we will focus on estimating a more general functional between 2 distributions, \mathcal{F} . We will show in Section 3 how \mathcal{F} generalises the $\alpha\beta$ -divergence, however, in principle there could be other divergences or functionals that \mathcal{F} generalises as well. For the rest of this section, we will formally define and discuss the problem of estimating the functional \mathcal{F} between 2 distributions using data sampled from these distributions.

Assume the existence of 2 jointly independent probability mass functions, $\mathbb{P} : \mathcal{X} \rightarrow [0, 1]$ and $\mathbb{Q} : \mathcal{X} \rightarrow [0, 1]$, over some common discrete domain, $\mathcal{X} = \bigotimes_{i=1}^k \mathcal{X}_i$ with $\text{dom}(X_i)$, comprised of all the possible value combinations over the common variables $\hat{X} = (X_1, \dots, X_k)$. Given 2 sets of samples from \mathbb{P} and \mathbb{Q} with size n and m respectively, consider the problem of estimating a functional, \mathcal{F} , between \mathbb{P} and \mathbb{Q} with the following form:

Definition 1. (Functional \mathcal{F})

$$\mathcal{F}(\mathbb{P}, \mathbb{Q}) = \sum_{\hat{x} \in \mathcal{X}} g[\mathbb{P}(\hat{x})]h[\mathbb{Q}(\hat{x})]L(g^*[\mathbb{P}(\hat{x})]h^*[\mathbb{Q}(\hat{x})])^l$$

where l is a binary valued parameter, $l \in \{0, 1\}$, L is any function with the property $L(\prod_x x) = \sum_x L(x)$, and g , h , g^* , and h^* are functions with the property $f(\prod_x x) = \prod_x f(x)$ for all $f \in \{g, h, g^*, h^*\}$.

The problem of estimating functional $\mathcal{F}(\mathbb{P}, \mathbb{Q})$ from samples of \mathbb{P} and \mathbb{Q} of size n and m respectively is fairly straightforward when n and m are large and the domain of \mathbb{P} and \mathbb{Q} , $|\mathcal{X}|$, is small [9, Theorem 8.11, Lemma 8.14]. However, this is not the case in the high-dimensional setting.

For instance, consider a naive plug-in approach to this problem where one first estimates the distributions \mathbb{P} and \mathbb{Q} from sample data, and then plugs in these estimates back into function \mathcal{F} to estimate $\mathcal{F}(\mathbb{P}, \mathbb{Q})$. Two issues can arise with this approach in the high-dimensional setting. This first issue occurs when n and m is small with respect to $|\mathcal{X}|$ which will cause a high variance when estimating the distributions \mathbb{P} and \mathbb{Q} from samples of these distributions. The other issue occurs when the number of variables in \mathbb{P} and \mathbb{Q} , k , is large. Since $|\mathcal{X}|$ grows exponentially with respect to k , and since \mathcal{F} contains a sum over $|\mathcal{X}|$, the time complexity of \mathcal{F} grows exponentially with respect to k . There are ways to avoid this exponential blow up, for instance, one could only consider the support of the estimates of \mathbb{P} and \mathbb{Q} which will bound the computation complexity by n and m . However,

this approach does not allow the use of various smoothing techniques such as basic additive smoothing and still does not solve the problem estimating distributions \mathbb{P} and \mathbb{Q} .

Therefore, in this paper we will propose a method for estimating the functional \mathcal{F} between 2 distributions that share a common domain using samples from them while avoiding the potential pitfalls stated earlier. We will then show how the proposed method can be used to estimate the $\alpha\beta$ -divergence between 2 distributions from sample data.

1.2 Contribution

The main contribution of this paper is the novel application of decomposable models to the problem of divergence estimation. The use of decomposable models allows the decomposition of the divergence estimation problem in high dimensions to smaller sub-problems in a lower dimension. In service of demonstrating the benefits of this approach, we develop a basic method that uses decomposable models for distribution estimation in a plug-in approach for divergence estimation. This method consists of 2 steps, estimating the population distributions from samples, and computing the divergence between these estimates in high dimensions.

The first step involves estimating the population distributions from samples of these distributions. There are already existing methods to learn decomposable models from data and these decomposable models will emit an estimate of the respective population distribution. Specifically, in this paper, we will use a software called "Chordalysis" [10], [11], [12], [13], however in principle we could use any other method to learn these decomposable models.

The second step involves computing the divergence between estimates of the population distributions given by the decomposable models. As stated in Section 1.1, we will use the $\alpha\beta$ -divergence in this paper, which is generalized by functional \mathcal{F} as we will show in Section 3. Therefore, this step will specifically involve computing the functional \mathcal{F} between estimates given by the decomposable models learnt from samples of the population distributions. Since there are no existing methods to do so, the secondary contribution of this paper will be a method to compute the functional \mathcal{F} between the joint distribution of 2 decomposable models.

A tertiary contribution of this paper is to show how functional \mathcal{F} from Definition 1 generalizes the $\alpha\beta$ -divergence.

2 NOTATION AND BACKGROUND

Let us summarize the notation and background necessary for the subsequent development.

2.1 Graphical Models

An undirected graph $G = (V, E)$ consists of $n = |V|$ vertices, connected via edges $(v, w) \in E$. For two graphs G_1, G_2 , we write $V(G_1)$ and $V(G_2)$ to denote the vertices of G_1 and G_2 , respectively and similar $E(G_1)$ and $E(G_2)$ for the edges. A clique C is a fully-connected subset of vertices, i.e., $\forall v, w \in C : (v, w) \in E$. The set of all cliques of G is denoted by \mathcal{C} . Here, any undirected graph represents the conditional independence structure of an undirected graphical model or Markov random field [14]. To this end, we identify each vertex $v \in V$ with a random variable

X_v taking values in the state space $\text{Dom}(X_v)$. The random vector $X = (X_v : v \in V)$, with probability mass function (pmf) $\hat{\mathbb{P}}$, represents the random joint state of all vertices in some arbitrary but fixed order, taking values \hat{x} in the Cartesian product space $\text{Dom}(X) = \bigotimes_{v \in V} \text{Dom}(X_v)$. If not stated otherwise, $\text{Dom}(X)$ is a discrete set. Moreover, we allow to access these quantities for any proper subset of variables $S \subset V$, i.e., $X_S = (X_v : v \in S)$, \hat{x}_S , and $\text{Dom}(X_S)$, respectively. We write C_{\max} for the clique C that has the largest state space $\text{Dom}(X_C)$. According to the Hammersley-Clifford theorem [6], the probability mass of $\text{Dom}(X)$ factorizes over positive functions $\psi_C : \text{Dom}(X) \rightarrow \mathbb{R}_+$, one for each maximal clique of the underlying graph,

$$\hat{\mathbb{P}}(X = \hat{x}) = \frac{1}{Z} \prod_{C \in \mathcal{C}} \psi_C(\hat{x}_C), \quad (1)$$

normalized via $Z = \sum_{\hat{x} \in \text{Dom}(X)} \prod_{C \in \mathcal{C}} \psi_C(\hat{x}_C)$. Due to positivity of ψ_C , it can be written as an exponential, i.e., $\psi_C(\hat{x}_C) = \exp(\langle \boldsymbol{\theta}_C, \phi_C(\hat{x}_C) \rangle)$ with sufficient statistic $\phi_C : \text{Dom}(X_C) \rightarrow \mathbb{R}^{|\text{Dom}(X_C)|}$. The overcomplete sufficient statistic of discrete data is a “one-hot” vector that selects a specific weight value, e.g., $\psi_C(\hat{x}_C) = \exp(\boldsymbol{\theta}_{C=\hat{x}_C})$. The full joint can be written in the famous exponential family form $\hat{\mathbb{P}}(X = \hat{x}) = \exp(\langle \boldsymbol{\theta}, \phi(\hat{x}) \rangle - \log Z)$ with $\boldsymbol{\theta} = (\boldsymbol{\theta}_C : C \in \mathcal{C})$ and $\phi(\hat{x}) = (\phi_C(\hat{x}_C) : C \in \mathcal{C})$.

The parameters of exponential family members are estimated by minimizing the negative average log-likelihood $\ell(\boldsymbol{\theta}; \mathcal{D}) = -(1/|\mathcal{D}|) \sum_{\hat{x} \in \mathcal{D}} \log \hat{\mathbb{P}}_{\boldsymbol{\theta}}(\hat{x})$ for some data set \mathcal{D} via first-order numeric optimization methods. \mathcal{D} contains samples from X , and it can be shown that the estimated probability mass converges to the data generating distribution as the size of \mathcal{D} increases. However, computing Z and hence performing probabilistic inference is #P-hard [15], [16]. Exact inference can be carried out via the junction tree algorithm. The junction tree representation of an undirected model is a tree, in which each vertex represents a maximal clique of a chordal completion of G [14, Sec. 2.5.2]. The cutset of each pair of adjacent clique-vertices is called separator.

Nevertheless, the junction tree requires that the underlying conditional independence structure of the graphical model is *decomposable*. Beside allowing for fast inference, another benefit of a decomposable model is that there is a closed form solution to the maximum likelihood parameter estimation problem for the joint distribution over all the variables in the model [17]. Given a decomposable model, \mathcal{M} , with n variables, the joint distribution can be written as $\hat{x} = \{x_1, \dots, x_n\} \in \mathcal{X}$, where the set \mathcal{X} is the Cartesian Product of the domain of each variable in \mathcal{M} , $\mathcal{X} = \text{Dom}(X_1) \times \dots \times \text{Dom}(X_n)$, is $\hat{\mathbb{P}}(\hat{x}) = \prod_{C \in \mathcal{C}} \hat{\mathbb{P}}_C(\hat{x}) / \prod_{S \in \mathcal{S}} \hat{\mathbb{P}}_S(\hat{x})$, where \mathcal{C} and \mathcal{S} is the set of maximal cliques and minimal separators in \mathcal{M} respectively, and where $\mathbb{P}_d(\cdot)$ represents the marginal probability over the domain d .

Decomposable models can be translated directly into an equivalent junction tree representation of the model. The junction tree of a decomposable model can be constructed by finding the minimum spanning tree of a “clique graph”, where each vertex of the clique graph is a maximal clique in the decomposable model and each edge is the separator between the vertex. The weight of each edge is then the

number of variables in the edge, or separator. The resulting junction tree will have vertex that are the maximal cliques, \mathcal{C}_{\max} , and edges that are the minimal separators, \mathcal{S} , of the decomposable model.

This also implies that we can represent $\hat{\mathbb{P}}$ as a product of conditional probability tables as well if we choose a random maximal clique in \mathcal{C} to be the root node of the tree.

2.2 Junction Tree Algorithm

Evaluating the partition function of loopy models exactly does not necessarily require a naive summation over the state space; there is another, more efficient, technique. Any loopy graph can be converted into a tree, the so-called *junction tree* (JT) [14], [18], [19]. As with BP in ordinary trees, inference on the junction tree has a time complexity that is polynomial in the maximal state space size of its vertices. The maximal vertex state space size of a junction tree is, however, exponential in the size of the largest clique of a triangulation² of G , a.k.a. exponential in the treewidth of G . Hence, if the treewidth of a loopy model is small, exact inference via the junction tree algorithm is rather efficient. Choosing a triangulation that results in a minimal treewidth is an NP-hard problem, but a valid triangulation can be found with time and memory complexity linear in the number of vertices [20], [21], [22]. Moreover, the maximal cliques of triangulated graphs can be computed in polynomial time w.r.t. to $|V|$ and $|\mathcal{N}_{\max}|$, i.e., the largest number of neighbors among all vertices. The actual computational complexity of inference on the junction tree can be computed directly from the vertex state spaces and the neighborhood sizes. When resources are limited, we can compute the junction tree, based on sub-optimal triangulation.

2.3 Divergence

Definition 2. (Divergence) Suppose S is the set of probability distributions with the same support. A divergence, D , is defined as $D(\cdot || \cdot) : S \times S \rightarrow \mathbb{R}$ such that $\forall \mathbb{P}, \mathbb{Q} \in S : D(\mathbb{P} || \mathbb{Q}) \geq 0$ and $\mathbb{P} = \mathbb{Q} \Leftrightarrow D(\mathbb{P} || \mathbb{Q}) = 0$.

Therefore, a divergence is not necessarily a distance metric as it does not need to be symmetric, i.e. $D(\mathbb{P} || \mathbb{Q}) = D(\mathbb{Q} || \mathbb{P})$, nor satisfy the triangle inequality.

Furthermore, there are also various generalized divergences, where many of the common divergences are special cases of the generalized divergence. An example of a popular generalized divergence is the Csiszár f-divergence. However, as stated in Section 1.1, in this paper we will use the generalized divergence known as the $\alpha\beta$ -divergence [8].

The $\alpha\beta$ -divergence, in Definition 3, has 2 parameters, α and β , that can be controlled to express other commonly used divergences. Specifically, the Kullback-Leibler divergence is obtained when $\alpha = 1, \beta = 0$, while the Hellinger distance is obtained when $\alpha = 0.5, \beta = 0.5$ [8].

Definition 3 ($\alpha\beta$ -divergence [8]). The $\alpha\beta$ -divergence, D_{AB} , between 2 positive measures \mathbb{P} and \mathbb{Q} is defined by the following, where α and β are parameters:

$$D_{AB}^{\alpha, \beta}(\mathbb{P}, \mathbb{Q}) = \sum_{\hat{x} \in \mathcal{X}} d_{AB}^{\alpha, \beta}(\mathbb{P}(\hat{x}), \mathbb{Q}(\hat{x})) \quad (2)$$

2. A triangulation of a graph $G = (V, E)$ is another graph $G' = (V, E')$ with $E \subseteq E'$, such that any induced cycle of G' has exactly three vertices.

where

$$d_{AB}^{(\alpha, \beta)}(\mathbb{P}(\hat{x}), \mathbb{Q}(\hat{x})) = \begin{cases} -\frac{1}{\alpha\beta} \left(\mathbb{P}(\hat{x})^\alpha \mathbb{Q}(\hat{x})^\beta - \frac{\alpha \mathbb{P}(\hat{x})^{\alpha+\beta}}{\alpha+\beta} - \frac{\beta \mathbb{Q}(\hat{x})^{\alpha+\beta}}{\alpha+\beta} \right) & \text{for } \alpha, \beta, \alpha + \beta \neq 0 \\ \frac{1}{\alpha^2} \left(\mathbb{P}(\hat{x})^\alpha \ln \frac{\mathbb{P}(\hat{x})^\alpha}{\mathbb{Q}(\hat{x})^\alpha} - \mathbb{P}(\hat{x})^\alpha + \mathbb{Q}(\hat{x})^\alpha \right) & \text{for } \alpha \neq 0, \beta = 0 \\ \frac{1}{\alpha^2} \left(\ln \frac{\mathbb{Q}(\hat{x})^\alpha}{\mathbb{P}(\hat{x})^\alpha} + \left(\frac{\mathbb{Q}(\hat{x})^\alpha}{\mathbb{P}(\hat{x})^\alpha} \right)^{-1} - 1 \right) & \text{for } \alpha = -\beta \neq 0 \\ \frac{1}{\beta^2} \left(\mathbb{Q}(\hat{x})^\beta \ln \frac{\mathbb{Q}(\hat{x})^\beta}{\mathbb{P}(\hat{x})^\beta} - \mathbb{Q}(\hat{x})^\beta + \mathbb{P}(\hat{x})^\beta \right) & \text{for } \alpha = 0, \beta \neq 0 \\ \frac{1}{2} (\ln \mathbb{P}(\hat{x}) - \ln \mathbb{Q}(\hat{x}))^2 & \text{for } \alpha, \beta = 0. \end{cases} \quad (3)$$

3 \mathcal{F} AND ITS RELATIONSHIP WITH $\alpha\beta$ -DIVERGENCES

In this section, we will show how by specifying the functions g, h, g^*, h^*, L , and binary variable l in the functional \mathcal{F} , we can obtain the various components in the $\alpha\beta$ -divergence. First, observe in Equation 3, that we can push the sum over \mathcal{X} into the various cases of $d_{AB}^{(\alpha, \beta)}$, resulting in Theorem 1.

Theorem 1. The 5 cases of the $\alpha\beta$ -divergence can be expressed in terms of 3 functionals:

$$\begin{aligned} f_1(\mathbb{P}, \mathbb{Q}; a, b) &= \sum_{\hat{x}} \mathbb{P}(\hat{x})^a \mathbb{Q}(\hat{x})^b \\ f_2(\mathbb{P}, \mathbb{Q}; a, b, c, d) &= \sum_{\hat{x}} \mathbb{P}(\hat{x})^a \mathbb{Q}(\hat{x})^b \ln(\mathbb{P}(\hat{x})^c \mathbb{Q}(\hat{x})^d) \\ f_3(\mathbb{P}, \mathbb{Q}) &= \frac{1}{2} \left(\sum_{\hat{x}} \ln \mathbb{P}(\hat{x}) - \sum_{\hat{x}} \ln \mathbb{Q}(\hat{x}) \right)^2 \end{aligned}$$

As stated in Section 1.2, we are interested in computing \mathcal{F} between 2 decomposable models. Therefore, for *just* this section, we assume that \mathbb{P} and \mathbb{Q} are distributions given by decomposable models $\mathcal{M}_{\mathbb{P}} = (\mathcal{G}_{\mathbb{P}}, \Phi_{\mathbb{P}})$ and $\mathcal{M}_{\mathbb{Q}} = (\mathcal{G}_{\mathbb{Q}}, \Phi_{\mathbb{Q}})$.

In order for the computation of the $\alpha\beta$ -divergence between \mathbb{P} and \mathbb{Q} to be viable, we need to show that it can be computed in a “tractable” manner. This follows if the same is the case for sub-functionals f_1 , f_2 , and f_3 . Here, we assume that the treewidth of $\mathcal{G}_{\mathbb{P}}$ and $\mathcal{G}_{\mathbb{Q}}$ are not too large as to render any computation with time complexity exponential with respect to the treewidth “intractable”.

Theorem 2. The time complexity for computing f_3 between 2 decomposable models is $\mathcal{O}(|\mathcal{C}(\mathcal{G}_{\mathbb{P}})|2^{\text{tw}(\mathcal{G}_{\mathbb{P}})}) + \mathcal{O}(|\mathcal{C}(\mathcal{G}_{\mathbb{Q}})|2^{\text{tw}(\mathcal{G}_{\mathbb{Q}})})$ where $\text{tw}(\mathcal{G})$ is the treewidth of \mathcal{G} .

Since computing f_3 can be done directly in a tractable manner, we then need a way to compute both f_1 and f_2 in a tractable manner, which unfortunately, cannot be done naively. However, if f_1 and f_2 can be expressed by \mathcal{F} , they can be computed using the method outlined in Section 4.

Theorem 3. Both f_1 and f_2 can be expressed by functional \mathcal{F} .

In conclusion, the $\alpha\beta$ -divergence between \mathbb{P} and \mathbb{Q} can be computed in a tractable manner either naively (when

$\alpha, \beta = 0$), or using the method outlined in Section 4. However, in some cases we might not have a decomposable model representation of \mathbb{P} and \mathbb{Q} . Therefore, using samples from \mathbb{P} and \mathbb{Q} , we will use the method outlined in Section 5 to estimate the $\alpha\beta$ -divergence between \mathbb{P} and \mathbb{Q} .

4 COMPUTING FUNCTIONAL \mathcal{F} BETWEEN DECOMPOSABLE MODELS

Recall the original problem of estimating the $\alpha\beta$ -divergence between \mathbb{P} and \mathbb{Q} using samples from them. In Section 1.2, we proposed a plug-in approach with 2 steps:

- 1) estimating \mathbb{P} and \mathbb{Q} using decomposable models, and
- 2) plugging in the estimates given by the decomposable models into the $\alpha\beta$ -divergence we wish to estimate.

In this section, we will provide details of a method that we will use to tackle the 2nd step of this plug-in approach while avoiding complexity exponential to the number of variables in \mathbb{P} and \mathbb{Q} , which will come with a naive approach.

In Section 3, we showed that the $\alpha\beta$ -divergence between 2 distributions can be expressed in terms of various parameterisations of the functional \mathcal{F} between these distributions. Therefore, in order to compute the $\alpha\beta$ -divergence between the estimates of \mathbb{P} and \mathbb{Q} given by the decomposable models, we just need a method to compute any parameterisation of the functional \mathcal{F} between these estimates.

The first logical step we can take would be to substitute the estimates, $\hat{\mathbb{P}}$ and $\hat{\mathbb{Q}}$, given by the decomposable models, $\mathcal{M}_{\mathbb{P}} = (\mathcal{G}_{\mathbb{P}}, \Phi_{\mathbb{P}})$ and $\mathcal{M}_{\mathbb{Q}} = (\mathcal{G}_{\mathbb{Q}}, \Phi_{\mathbb{Q}})$, into the general form of functional \mathcal{F} from Definition 1.

$$\begin{aligned} \mathcal{F}(\hat{\mathbb{P}}, \hat{\mathbb{Q}}) &= \sum_{\hat{x} \in \mathcal{X}} g\left[\hat{\mathbb{P}}(\hat{x})\right] h\left[\hat{\mathbb{Q}}(\hat{x})\right] L\left(g^*\left[\hat{\mathbb{P}}(\hat{x})\right] h^*\left[\hat{\mathbb{Q}}(\hat{x})\right]\right)^l \\ &= \sum_{C \in \mathcal{C}(\mathcal{G}_{\mathbb{P}})} \sum_{\hat{x}_C \in \mathcal{X}_C} L\left(g^*\left[\hat{\mathbb{P}}_C^{\text{JT}}(\hat{x}_C)\right]\right)^l SP_C(\hat{x}_C) \\ &\quad \sum_{C \in \mathcal{C}(\mathcal{G}_{\mathbb{Q}})} \sum_{\hat{x}_C \in \mathcal{X}_C} L\left(h^*\left[\hat{\mathbb{Q}}_C^{\text{JT}}(\hat{x}_C)\right]\right)^l SP_C(\hat{x}_C) \end{aligned} \quad (4)$$

Where $\mathbb{P}_C^{\text{JT}}(\hat{x}_C) = \mathbb{P}(\hat{x}_{C-\text{pa}(C)} | \hat{x}_{\text{pa}(C)})$ for $C \subset \hat{X}$: $\mathbb{P}_C^{\text{JT}}(\hat{x}_{\hat{X}}) = \mathbb{P}_C^{\text{JT}}(\hat{x}_C)$ and $\text{pa}(C)$ is the parent of the maximal clique C in the junction tree JT of $\hat{\mathbb{P}}$'s and $\hat{\mathbb{Q}}$'s respective chordal graph. Moreover

$$\begin{aligned} SP_C(\hat{x}_C) &= \sum_{\hat{x} \in \mathcal{X}_{\hat{X}-C}} g\left[\hat{\mathbb{P}}(\hat{x}_C, \hat{x})\right] h\left[\hat{\mathbb{Q}}(\hat{x}_C, \hat{x})\right] \\ &= \sum_{\hat{x} \in \mathcal{X}_{\hat{X}-C}} \left[\prod_{C \in \mathcal{C}_{\mathbb{P}}} g\left[\hat{\mathbb{P}}_C^{\text{JT}}(\hat{x})\right] \right] \left[\prod_{C \in \mathcal{C}_{\mathbb{Q}}} h\left[\hat{\mathbb{Q}}_C^{\text{JT}}(\hat{x})\right] \right] \end{aligned} \quad (5)$$

This equality holds due to a combination of the property of functions g^* and h^* detailed in Definition 1, a basic property of the logarithmic function L , the fact that parameter l can only be either 0 or 1, and the associativity of summations.

Remark 1. The lower bound complexity of naively computing Equation 4 is $\Omega(2^{|\hat{X}|})$ where $|\hat{X}|$ is the number of variables. Therefore naively computing the functional \mathcal{F} between 2 high dimensional decomposable models is intractable.

Therefore, we will provide details of a general method for computing $\mathcal{F}(\hat{\mathbb{P}}, \hat{\mathbb{Q}})$ in a more tractable manner. This

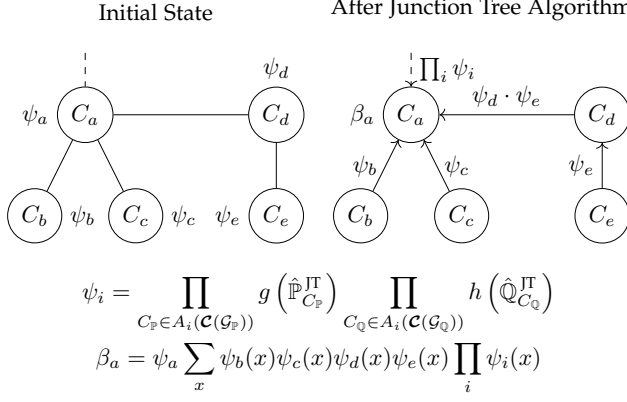


Fig. 2. Junction Tree Algorithm to compute the functional \mathcal{F} between 2 decomposable models $\mathcal{M}_{\mathbb{P}}$ and $\mathcal{M}_{\mathbb{Q}}$ using computation graph \mathcal{H} . We also assume the computation graph \mathcal{H} is fully connected.

method, which we will refer to as a Junction Forest Computation (JFComp), requires knowledge of a *computation graph*, \mathcal{H} , between decomposable models $\mathcal{M}_{\mathbb{P}}$ and $\mathcal{M}_{\mathbb{Q}}$.

Definition 4 (strictly larger, clique mapping α). A chordal graph \mathcal{H} is *strictly larger* than chordal graphs $\mathcal{G}_{\mathbb{P}}$ and $\mathcal{G}_{\mathbb{Q}}$ if all the maximal cliques in both chordal graphs is either a subset or equal to a maximal clique in \mathcal{H} . In other words, \mathcal{H} is *strictly larger* than $\mathcal{G}_{\mathbb{P}}$ and $\mathcal{G}_{\mathbb{Q}}$ if and only if there exists a mapping α such that:

$$\begin{aligned} \alpha : \mathcal{C}(\mathcal{G}_{\mathbb{P}}, \mathcal{G}_{\mathbb{Q}}) &\rightarrow \mathcal{C}(\mathcal{H}) \\ \text{s.t. } \forall C \in \mathcal{C}(\mathcal{G}_{\mathbb{P}}, \mathcal{G}_{\mathbb{Q}}) : C &\subseteq \alpha(C) \end{aligned}$$

where $\mathcal{C}(\mathcal{G}_{\mathbb{P}}, \mathcal{G}_{\mathbb{Q}}) = \mathcal{C}(\mathcal{G}_{\mathbb{P}}) \cup \mathcal{C}(\mathcal{G}_{\mathbb{Q}})$ is the set of maximal cliques in chordal graphs $\mathcal{G}_{\mathbb{P}}$ and $\mathcal{G}_{\mathbb{Q}}$.

Definition 5 (computation graph). If a chordal graph, \mathcal{H} , is *strictly larger* than chordal graphs $\mathcal{G}_{\mathbb{P}}$ and $\mathcal{G}_{\mathbb{Q}}$, then \mathcal{H} is a *computation graph* of decomposable models $\mathcal{M}_{\mathbb{P}} = (\mathcal{G}_{\mathbb{P}}, \Phi_{\mathbb{P}})$ and $\mathcal{M}_{\mathbb{Q}} = (\mathcal{G}_{\mathbb{Q}}, \Phi_{\mathbb{Q}})$.

We will discuss a simple way one might obtain such a chordal graph, \mathcal{H} , in conjunction with models $\mathcal{M}_{\mathbb{P}}$ and $\mathcal{M}_{\mathbb{Q}}$ using samples from \mathbb{P} and \mathbb{Q} in Section 5.

Definition 6 (A, cliques assigned by α to C). Assume we have the clique mapping $\alpha : \mathcal{C}(\mathcal{G}_{\mathbb{P}}, \mathcal{G}_{\mathbb{Q}}) \rightarrow \mathcal{C}(\mathcal{H})$. Then we define a function, A , to obtain the maximal cliques in chordal graphs $\mathcal{G}_{\mathbb{P}}$ and $\mathcal{G}_{\mathbb{Q}}$ assigned by α to some maximal clique in \mathcal{H} :

$$\begin{aligned} A : \mathcal{C}(\mathcal{H}) &\rightarrow (\mathcal{P}(\mathcal{C}(\mathcal{G}_{\mathbb{P}}, \mathcal{G}_{\mathbb{Q}})) \rightarrow \mathcal{P}(\mathcal{C}(\mathcal{G}_{\mathbb{P}}, \mathcal{G}_{\mathbb{Q}}))) \\ \text{s.t. } \forall C \in \mathcal{C}(\mathcal{H}) : A_C(C) &= \{C' : C' \in \mathcal{C} \wedge C' \subseteq C\} \end{aligned}$$

where $\mathcal{P}(S)$ is the powerset of set S .

For the rest of this section, we will provide details on how JFComp uses Junction Tree Algorithms, as described in Section 2.2, to compute the functional \mathcal{F} between 2 decomposable models. In Subsection 4.1, we will first provide details on how JFComp works when the computation graph, \mathcal{H} , is a fully connected graph. We refer to JFComp as Junction Tree Computation (JTComp) with this restriction. We then show how this can be extended to handle a disconnected \mathcal{H} in Subsection 4.2. This will fully describe DeMoDivEst.

4.1 Junction Tree Computation (JTComp)

Recall we want to compute $\mathcal{F}(\hat{\mathbb{P}}, \hat{\mathbb{Q}})$ as expressed in Equation 4. Observe that the 2 nested sums in $\mathcal{F}(\hat{\mathbb{P}}, \hat{\mathbb{Q}})$ has innermost sums with domains of similar forms but over different sets of maximal cliques, $\mathcal{C}(\mathcal{G}_{\mathbb{P}})$ and $\mathcal{C}(\mathcal{G}_{\mathbb{Q}})$ respectively. Therefore, using Theorem 4, we can re-express $\mathcal{F}(\hat{\mathbb{P}}, \hat{\mathbb{Q}})$ such that the innermost sum of both nested sums are of the same form and over the same set of maximal cliques, $\mathcal{C}(\mathcal{H})$.

Theorem 4. Assume we have 2 decomposable models $\mathcal{M}_{\mathbb{P}}$ and $\mathcal{M}_{\mathbb{Q}}$ and a computation graph \mathcal{H} for both models. By Definition 4, we also have a mapping α from maximal cliques in $\mathcal{M}_{\mathbb{P}}$ and $\mathcal{M}_{\mathbb{Q}}$ to maximal cliques in \mathcal{H} . Then the following equivalences holds:

$$\sum_{C \in \mathcal{C}(\mathcal{G}_{\mathbb{P}})} \sum_{\hat{x}_C \in \mathcal{X}_C} L\left(g^* \left[\hat{\mathbb{P}}_C^{\text{JT}}(\hat{x}_C)\right]\right)^l SP_C(\hat{x}_C) \quad (6)$$

$$= \sum_{C \in \mathcal{C}(\mathcal{G}_{\mathbb{P}})} \sum_{\hat{x}_{\alpha(C)} \in \mathcal{X}_{\alpha(C)}} L\left(g^* \left[\hat{\mathbb{P}}_C^{\text{JT}}(\hat{x}_{\alpha(C)})\right]\right)^l SP_{\alpha(C)}(\hat{x}_{\alpha(C)})$$

$$\sum_{C \in \mathcal{C}(\mathcal{G}_{\mathbb{Q}})} \sum_{\hat{x}_C \in \mathcal{X}_C} L\left(h^* \left[\hat{\mathbb{Q}}_C^{\text{JT}}(\hat{x}_C)\right]\right)^l SP_C(\hat{x}_C) \quad (7)$$

$$= \sum_{C \in \mathcal{C}(\mathcal{G}_{\mathbb{Q}})} \sum_{\hat{x}_{\alpha(C)} \in \mathcal{X}_{\alpha(C)}} L\left(h^* \left[\hat{\mathbb{Q}}_C^{\text{JT}}(\hat{x}_{\alpha(C)})\right]\right)^l SP_{\alpha(C)}(\hat{x}_{\alpha(C)})$$

Thanks to Theorem 4, the domain of any instance of $SP_{\alpha(C)}$ is a maximal clique in the \mathcal{H} . Therefore, as Theorem 5 will state, we can use junction tree algorithms to compute $SP_{\alpha(C)}$ in time exponential to the treewidth of graph \mathcal{H} instead of time exponential to the number of variables in $\hat{X} - \alpha(C)$. An illustration of this procedure can be found in Figure 2.

Theorem 5. Given 2 decomposable models, $\mathcal{M}_{\mathbb{P}}$ and $\mathcal{M}_{\mathbb{Q}}$, and a computation graph of both models, \mathcal{H} . Let Φ be a set of factors defined as follows:

$$\Phi := \left\{ g \circ \hat{\mathbb{P}}_{C_{\mathbb{P}}}^{\text{JT}} : C_{\mathbb{P}} \in \mathcal{C}(\mathcal{G}_{\mathbb{P}}) \right\} \cup \left\{ h \circ \hat{\mathbb{Q}}_{C_{\mathbb{Q}}}^{\text{JT}} : C_{\mathbb{Q}} \in \mathcal{C}(\mathcal{G}_{\mathbb{Q}}) \right\}$$

After running the junction tree algorithm over chordal graph \mathcal{H} with factors Φ , we will get the following beliefs over each maximal clique in \mathcal{H} :

$$\forall C \in \mathcal{C}(\mathcal{H}) : \beta_C(\hat{x}_C) = SP_C(\hat{x}_C)$$

Therefore, using the junction tree algorithm, we obtain beliefs over each maximal clique in the chordal graph \mathcal{H} that we can use to substitute for SP in Equation 4:

$$\begin{aligned} \mathcal{F}(\hat{\mathbb{P}}, \hat{\mathbb{Q}}) &= \sum_{C \in \mathcal{C}(\mathcal{G}_{\mathbb{P}})} \sum_{\hat{x}_{\alpha(C)} \in \mathcal{X}_{\alpha(C)}} L\left(g^* \left[\hat{\mathbb{P}}_C^{\text{JT}}(\hat{x}_{\alpha(C)})\right]\right)^l \beta_{\alpha(C)}(\hat{x}_{\alpha(C)}) + \\ &\quad \sum_{C \in \mathcal{C}(\mathcal{G}_{\mathbb{Q}})} \sum_{\hat{x}_{\alpha(C)} \in \mathcal{X}_{\alpha(C)}} L\left(h^* \left[\hat{\mathbb{Q}}_C^{\text{JT}}(\hat{x}_{\alpha(C)})\right]\right)^l \beta_{\alpha(C)}(\hat{x}_{\alpha(C)}) \quad (8) \end{aligned}$$

Corollary 1 will show that the complexity of computing the expression in Equation 8, and therefore the complexity of using JTComp to compute \mathcal{F} between 2 decomposable models, is $\mathcal{O}(|\mathcal{C}(\mathcal{G}_{\mathbb{P}})| + |\mathcal{C}(\mathcal{G}_{\mathbb{Q}})| \cdot 2^{\text{tw}(\mathcal{G})})$. Therefore, using JTComp to compute \mathcal{F} between 2 decomposable models

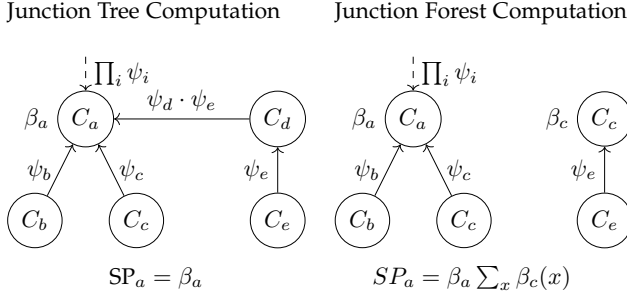


Fig. 3. Differences in getting the clique beliefs over each maximal clique in the computation graph \mathcal{H} between a fully connected and a disconnected computation graph

should be more efficient than computing it naively when the computational graph \mathcal{H} is not a fully saturated graph.

Corollary 1 (Complexity of Junction Tree Computation (JTComp)). Computing the functional $\mathcal{F}(\hat{\mathbb{P}}, \hat{\mathbb{Q}})$ using JTComp has time complexity $\mathcal{O}(|\mathcal{C}(\mathcal{G}_{\mathbb{P}})| + |\mathcal{C}(\mathcal{G}_{\mathbb{Q}})| \cdot 2^{\text{tw}(\mathcal{H})})$, where $\text{tw}(\mathcal{H})$ is the treewidth of the chordal graph \mathcal{H} .

4.2 Junction Forest Computation (JFCOMP)

In Section 4.1, we assumed that the computation graph for decomposable models $\mathcal{M}_{\mathbb{P}}$ and $\mathcal{M}_{\mathbb{Q}}$, \mathcal{H} is fully connected. However, this might not always be the case. In this section, we will show how the methods in Section 4.1 can be extended to handle cases where \mathcal{H} is disconnected.

When the computation graph \mathcal{H} is disconnected, \mathcal{H} can be represented as a list of chordal graphs, $\mathcal{H} = \{\mathcal{H}_i\}$. Therefore, we also have a list of junction trees for each chordal graph in \mathcal{H} , $\mathcal{T} = \{\mathcal{T}_i\}$, as well.

Since the disconnected computation graph, \mathcal{H} , is still strictly larger than the chordal graph structure of $\mathcal{M}_{\mathbb{P}}$ and $\mathcal{M}_{\mathbb{Q}}$, by Definition 4, there is still a mapping α from maximal cliques in $\mathcal{M}_{\mathbb{P}}$ and $\mathcal{M}_{\mathbb{Q}}$ to maximal cliques in \mathcal{H} . However, since chordal graph \mathcal{H} is now comprised of multiple chordal graphs, and therefore junction trees, we are unable to apply Theorem 5 directly to compute SP from Equation 5. The reason for this is because there is no single junction tree to run the junction tree algorithm on, therefore factors from different junction trees are unable to propagate to each other.

Instead, we show in Theorem 6, that having a disconnected computation graph \mathcal{H} , and therefore a set of junction trees, \mathcal{T} , which are disconnected from each other, essentially breaks up SP into smaller sub-problems over each junction tree in \mathcal{T} . The results of these sub-problems can then be combined to compute SP . An illustration of the result from Theorem 6 and its difference in computing SP on a fully connected computational graph can be found in Figure 3.

Definition 7 (τ , clique to junction tree mapping). Assume we have 2 decomposable models, $\mathcal{M}_{\mathbb{P}}$ and $\mathcal{M}_{\mathbb{Q}}$, with chordal graph structures $\mathcal{G}_{\mathbb{P}}$ and $\mathcal{G}_{\mathbb{Q}}$. Also assume we have a computation graph, \mathcal{H} , for $\mathcal{M}_{\mathbb{P}}$ and $\mathcal{M}_{\mathbb{Q}}$ that is a disconnected graph. As such, \mathcal{H} has a junction forest representation comprising of junction trees in the set \mathcal{T} .

Let τ be a mapping from the maximal cliques of $\mathcal{M}_{\mathbb{P}}$ and $\mathcal{M}_{\mathbb{Q}}$ to a junction tree in \mathcal{T} that contains the maximal clique given by the clique mapping, α , from Definition 4:

$$\begin{aligned} \tau : \mathcal{C}(\mathcal{G}_{\mathbb{P}}) \cup \mathcal{C}(\mathcal{G}_{\mathbb{Q}}) &\rightarrow \mathcal{T} \\ \text{s.t. } \forall C \in \mathcal{C}(\mathcal{G}_{\mathbb{P}}) \cup \mathcal{C}(\mathcal{G}_{\mathbb{Q}}) : \alpha(C) &\in \mathcal{C}(\tau(C)) \end{aligned}$$

Theorem 6. If the computation graph \mathcal{H} for decomposable models $\mathcal{M}_{\mathbb{P}}$ and $\mathcal{M}_{\mathbb{Q}}$ is disconnected, $SP_{\alpha(C)}$ in Equation 6 and 7 can be re-expressed as follows:

$$\begin{aligned} SP_{\alpha(C)}(\hat{x}_{\alpha(C)}) &= \beta_{\alpha(C)}(\hat{x}_{\alpha(C)}) \prod_{\mathcal{T}_i \in \mathcal{T} - \tau(C)} \sum_{\hat{x} \in \mathcal{X}_{C(\mathcal{T}_i)}} \beta_{C(\mathcal{T}_i)}(\hat{x}_{\alpha(C)}, \hat{x}) \end{aligned}$$

where $C(\mathcal{T}_i)$ represents any clique in the set of maximal cliques in junction tree \mathcal{T}_i .

This insight has significant implications for the computational complexity of our approach. All we need to do to obtain the required beliefs is to run the junction tree algorithm for each junction tree in \mathcal{T} separately. Moreover, we are allowed to use the same clique mapping α from Definition 4 to assign the factors in Φ to cliques in the junction trees of \mathcal{T} .

Once the computation for each junction tree in \mathcal{T} is finished, we can compute $SP_{\alpha(C)}(\hat{x}_{\alpha(C)})$ for all $C \in \mathcal{C}(\mathcal{G}_{\mathbb{P}}, \mathcal{G}_{\mathbb{Q}})$. Therefore, even if the computation graph \mathcal{H} is disconnected and chordal, we can compute SP and thus $\mathcal{F}(\mathbb{P}, \mathbb{Q})$.

5 ESTIMATING $\alpha\beta$ -DIVERGENCE

Recall from Section 1.1 that the main problem we wish to tackle is the estimation of the $\alpha\beta$ -divergence, as defined in Definition 3, between distributions \mathbb{P} and \mathbb{Q} using only samples from \mathbb{P} and \mathbb{Q} .

As stated in Section 1.2, we will approach this problem via a plug-in approach. Taking everything we have discussed so far into account, a more detailed version of the steps in this plug-in approach is as follows:

- 1) Learn 2 decomposable models in conjunction with their shared computation graph, \mathcal{H} , from the samples of \mathbb{P} and \mathbb{Q} respectively.
- 2) Compute the $\alpha\beta$ -divergence between the 2 decomposable models either directly or by computing the needed parameterisations of the functional \mathcal{F} between these decomposable models.

We will refer to this specific approach as the Decomposable Model Divergence Estimator (DeMoDivEst).

It is clear why Step 2 is the case and how it can be achieved from Section 3 and 4. But to reiterate, we showed in Section 3, in cases where naive computation of the $\alpha\beta$ -divergence between 2 decomposable models is intractable, we can express the $\alpha\beta$ -divergence in terms of different parameterisations of the functional \mathcal{F} . The different parameterisations of \mathcal{F} needed to express the $\alpha\beta$ -divergence depends on the specific $\alpha\beta$ -divergence we wish to estimate. Therefore, instead of computing the $\alpha\beta$ -divergence between 2 decomposable models directly, we can compute the needed parameterisations of \mathcal{F} between these decomposable models to the same end. This computation step can be done using the method JFCOMP outlined in Section 4,

However, achieving Step 1 is still unclear. Specifically, it is still unclear how we might obtain the computation graph \mathcal{H} , in conjunction with learning the decomposable models from samples of \mathbb{P} and \mathbb{Q} .

In this paper we will use a straightforward approach to obtain the computation graph in conjunction with the decomposable models estimating distributions \mathbb{P} and \mathbb{Q} . Specifically, we will learn the computation graph first by pooling the samples from both distributions together and using Chordalysis-SMT [10], [12], [13] to learn a chordal graph structure on this pooled dataset. We then use this chordal graph learnt on the pooled dataset as the computation graph \mathcal{H} . Furthermore, we will also use this chordal graph as the graphical structure of the decomposable models estimating the distributions \mathbb{P} and \mathbb{Q} . After fixing the structure of these 2 decomposable models, we then learn the parameters of these decomposable models on samples from distributions \mathbb{P} and \mathbb{Q} respectively.

However, this approach may result in decomposable models with inaccurate structures because the variable structure can change due to concept drift. Ideally the decomposable models for the 2 distributions would be allowed to differ in structure. The methods we have developed can accommodate such differences in structure, so long as there is an appropriate method for finding a computation graph for the 2 decomposable models. We leave the problem of creating a method to achieve this to future research.

6 RELATED WORK

Estimating the divergence between 2 high dimensional discrete distributions, \mathbb{P} and \mathbb{Q} , with limited samples is a problem that has been addressed by a number of previous approaches [23], [24], [25], [26], [27], [28], [29]. Unfortunately, using naive approaches to tackle this problem tend to perform poorly due to the reasons outlined in Section 1.1. Fortunately, there has been some effort into developing methods to carry out such divergence estimation.

A naive way to approach divergence estimation would be to use a plug-in approach where the population distributions are estimated using the empirical distribution, and these estimates are plugged in to the divergence we wish to estimate. However, instead of using the empirical distribution, it might be better to use a more sample efficient method for estimating the distributions \mathbb{P} and \mathbb{Q} in high-dimensional scenarios. One such way is to use the Profile Maximum Likelihood (PML) to estimate the distributions \mathbb{P} and \mathbb{Q} . The PML estimator maximises likelihood of observing the number of unique symbols appearing the amount of times within a dataset and better explains the data than standard Maximum Likelihood when the number of symbols is large compared to the size of the given dataset [30]. It was later shown that a PML based approach is competitive for estimating any symmetric property of a collection of distributions, such as the $\alpha\beta$ -divergence [23]. However, since the PML is difficult to compute exactly, approximations of the PML have been proposed that have been showed empirically to be competitive to existing divergence estimation approaches [24].

Another approach to divergence estimation is to create an estimator of the target divergence. One work has

shown that using a plug-in approach with the empirical distribution yields infinite bias error while the estimator they proposed has an exponentially decaying bias [25]. More recently, a prominent approach to creating divergence estimators is the use of polynomial approximations of the divergence. One general approach that has been proposed is to identify “smooth” and “non-smooth” regimes of the divergence. This approach then uses a version of a bias-corrected Maximum Likelihood Estimator for estimation in the “smooth” regime while using a polynomial approximation in the “non-smooth” regime [26]. This general approach can be used for estimating the Kullback-Leibler divergence, Hellinger distance, and χ^2 -divergence [26]. A similar approach was proposed for estimating the Kullback-Leibler divergence with the main difference being the use of an bias-corrected augmented plug-in estimator in the “smooth” regime [28]. This approach was also used for tackling the problem of estimation the Total Variation Distance (L_1 Distance) with the main difference being the use of a 2-dimensional polynomial approximation to approximate the L_1 Distance in the “non-smooth” regime instead of just the best 1-dimensional polynomial approximation [29].

One issue with the polynomial approximation approaches discussed is that they require splitting the available sample into 2 or more parts, the first for regime classification and the rest for estimation. Therefore, these polynomial approximation approaches don’t fully use all the samples for estimation. Recently, a method was proposed that used do not require splitting the sample in order to carry out regime classification. This method solves a problem-independent linear program based on moment matching to carry out estimation in the “non-smooth” regime while using a problem-dependent bias-corrected plug-in estimator in the “smooth” regime [27].

7 EXPERIMENTS

In order to empirically assess the usefulness of our proposed approach for divergence estimation, we will run 2 types of experiments. In Section 7.2, we will compare DeMoDivEst against various existing methods for divergence estimation using synthetic data generated from the generator described in Section 7.1. This will show how a basic implementation of the proposed approach measures up to existing methods for divergence estimation. Then in Section 7.3, we will study how the behaviour of DeMoDivEst changes under varying configurations of the distributions we wish to estimate the divergence between and the amount of samples available.

7.1 Data Generator

In order to run the experiments throughout the rest of Section 7, we require datasets that have data sampled from distributions with a known amount of divergence between them. Due to the lack of abundance of such high dimensional datasets, we decided to use a synthetic dataset generator, such that each generated dataset pair (the datasets before and after drift) will contain data sampled from 2 distributions with a known divergence between them.

Creating such a generator, especially one that can generate high-dimensional datasets, is a problem in and on itself.

TABLE 1

Divergence estimation methods that have existing implementations that we will compare against. An implementation of our proposed approach and everything else needed to reproduce the experiments in this paper can be found online at <https://gitlab.com/lklee/divergence-estimation-via-graphical-models>.

Method	Description	Reference
zg	estimator for KL divergence	[25]
bzlv	polynomial approximation	[28]
hjw	polynomial approximation	[26]
jfc_tw=n	our proposed method but with a limit to the treewidth of the decomposable model of n	-

One way to approach this problem is to create 2 generative models representing the 2 distributions the dataset pair will be sampled from. These generative models should be created such that the divergence between the 2 distributions matches some given target. Therefore, in order for a generator using this approach to be viable, we need to use a class of generative models with a tractable method for computing some divergence between 2 models under this class.

However, it is not a given that there is a tractable method, with respect to the number of variables, for computing the divergence between 2 models under any class of generative models. However, we at least do know of such a method for decomposable models as described in Section 4, and therefore will use them to represent the distributions we sample from in our synthetic data generator. We will call this synthetic data generator the Decomposable Model Generator (DeMoGen). Ideally, we would use another class of generative models for this purpose in order to increase the fairness of the comparison experiments in Section 7.2, however, developing a method to measure a divergence under another class of generative models is out of scope of this paper. Therefore, in order to slightly compensate for this source of unfairness, we will limit the treewidth of the decomposable models used by DeMoDivEst. By limiting the treewidth of the decomposable models learnt from the sampled data, we can observe how DeMoDivEst behaves when the learnt decomposable models cannot accurately model the original population distributions.

For the experiments in this section, we will use DeMoGen to create 50 datasets pairs for each combination of the parameters below. To be clear, the generator measures the true divergence between the 2 generating models while the estimators estimates that divergence from data generated from those models.

Hellinger Distance 0.1, 0.3, 0.5, 0.7, 0.9

Number of Binary Variables 10, 15, 20, 30, 40, 50, 100

Treewidth 3, 5, 7, 9

Each dataset pair, representing data sampled from 2 distributions with a given Hellinger Distance between them, will contain 100,000 samples from each distribution, totaling to 200,000 samples over both datasets in each pair.

The reason we use Hellinger Distance as the target divergence is due it being bounded between 0 and 1, as opposed to the Kullback-Leibler Divergence which is unbounded. By having a fixed scale, we are able to ensure that the datasets

we generate cover the entire range of possible Hellinger Distances. This should allow for our experiments to have more coverage and be more systematic. Furthermore, by having a fixed range of values, and therefore a somewhat universal meaning for any value of the Hellinger Distance, we are able to compare estimation results across datasets of different configurations by focusing on specific values of Hellinger Distances in the analysis of the results.

However, since we will compare DeMoDivEst against the other methods in Table 1 at estimating the Symmetric KL Divergence, $KL(P||Q) + KL(Q||P)$, we will need the true Symmetric KL Divergence between the 2 population distributions of each dataset pair. Therefore, during the data generation process, we measure and record the exact Symmetric KL Divergence between the decomposable models from which the dataset pairs are generated from. We also measure the exact Hellinger Distance between the decomposable models during generation as well for use in Section 7.3.

7.2 Comparison with Other Methods

In this section we will compare the method proposed in this paper with various existing methods for estimating the divergence between 2 distributions using sample data. Specifically we will compare DeMoDivEst against the methods in Table 1, all of which has been described in Section 6, in estimating the symmetric Kullback-Leibler Divergence between datasets in each dataset pair described in Section 7.1. We use the KL Divergence in this comparison due to some of the methods in Table 1 only having implementations that estimate the KL Divergence. We also use the symmetric version of the KL Divergence to prevent any confusion on which of the 2 distributions is P and which is Q .

It is important to reiterate that since both DeMoGen and DeMoDivEst uses decomposable models to represent probability distributions, it is possible for the results of this comparison experiment to be biased in favour of DeMoDivEst. Unfortunately, this is a problem that cannot be remedied in scenarios where the number of variables is large due to an absence of data generators capable of generating the required data. Therefore, the following results should be taken in with this fact in mind.

The results of the comparison between DeMoDivEst and the methods in Table 1 can be found in Figure 4. These results were obtained using all of the data available in each dataset, that is to say each method is given 100,000 samples from each of the 2 distributions to estimate the symmetric KL-divergence between them. Furthermore, there are 2 plots in Figure 4, each representing results with DeMoGen of different treewidths, specifically treewidths of size 5 and 7.

The first thing should take note of in Figure 4 is that distribution of points along the x-axis becomes increasingly concentrated at certain points as the number of variables increases. Specifically, when the number of variables is 100, there are 5 clusters along the x-axis which seems to correspond to the 5 levels of Hellinger Distance used during the generation of the datasets in Section 7.1. It then seems probable that the high variability of the generated symmetric KL-divergence at low dimensions is due to inadequacies in generating datasets matching the 5 specified Hellinger

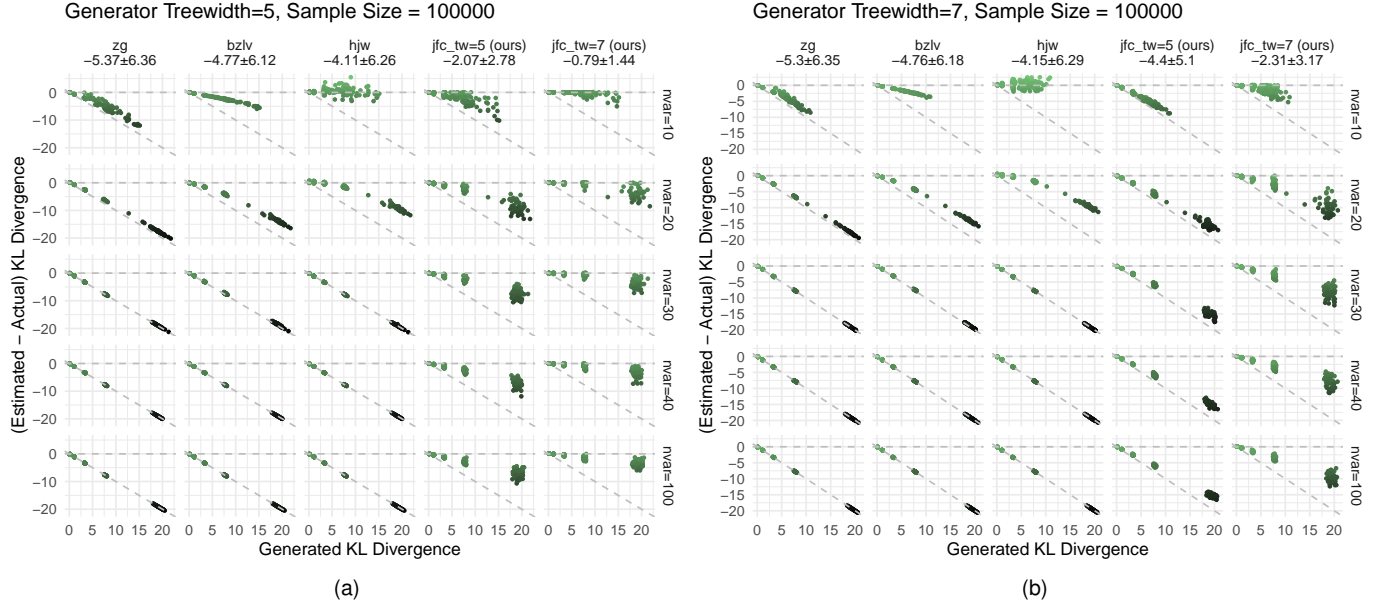


Fig. 4. Comparison of DeMoDivEst with various methods in Section 6. Each plot, comprised of multiple subplots, represents results from different treewidths (i.e. (a)5 and (b)7) for DeMoGen. The columns of each plot represents the various methods being compared against, each row represents differing number of binary variables. The x-axis of each subplot represents the symmetric KL-divergence generated, the y-axis represents the estimated minus true symmetric KL divergence. Points above and below the y-axis represents over and under estimation respectively. The line $y = -x$ represents maximum amount of underestimation error (when estimate given is 0).

Distances at low dimensions. This inadequacy is likely due to a lack of parameters in the decomposable models to manipulate in order to achieve the target Hellinger Distance.

On the surface, we can observe from Figure 4 that the method zg seems to severely underestimate the symmetric KL divergence between the distributions, giving estimates close to 0, even for datasets containing 10 binary variables. On the other hand, $bzlv$ gives estimates that outperforms zg but still clearly underestimates the symmetric KL divergence at 10 binary variables. Out of all the existing methods in Table 1, hhw performs the best, and also does not clearly underestimate the KL divergence when the number of binary variables is 10. As the number of binary variables increases, these 3 existing methods start to increasingly underestimate the symmetric KL divergence. Specifically, these methods start returning estimates close of 0 when the number of binary variables is 30.

In terms of how DeMoDivEst performed, we can observe that the error for $jfc_tw=5$ and $jfc_tw=7$ does not increase with respect to the number of binary variables in the datasets. Instead the error for both $jfc_tw=5$ and $jfc_tw=7$ increases as the treewidth of the data generator DeMoGen increases. We can also observe from $jfc_tw=7$'s results in Figure 4a that DeMoDivEst preforms very well when the treewidth limit of DeMoDivEst is slightly higher than the treewidth of the dataset's underlying distribution.

When the dimensionality is low (i.e. number of variables is 10 or 20), the existing methods, zg , $bzlv$, and hhw , give some of the most accurate estimates, regardless of the treewidth of DeMoGen. On the other hand, the results for our method, DeMoDivEst, on low dimensions is a bit of a mixed bag. In low dimensions, the existing methods are more accurate than DeMoDivEst whenever the treewidth is limited to be less than that of the generating distributions.

However, even when that is not the case, DeMoDivEst performs slightly worse than hhw when the number of variables is 10.

Where our method, DeMoDivEst, performs significantly better than the other methods is when dimensionality is high (i.e. where the number of variables is ≥ 30). As we can observe from Figure 4, when dimensionality is high, zg , hhw , and $bzlv$ start to return estimates that are close to 0. Conversely, a similar issue only occurs in DeMoDivEst when the treewidth limit given to DeMoDivEst is about 2 binary variables fewer than the treewidth of the source distribution. But even then, DeMoDivEst is still slightly more accurate than zg , hhw , and $bzlv$.

7.3 Scalability and Convergence

As stated in Section 1.2, one of the main goals of our proposed method, DeMoDivEst, is to estimate $\alpha\beta$ -divergences from sample data while scaling well with respect to the number of variables in the population distribution. Therefore, in this section we will specifically study how DeMoDivEst scales with respect to the dimensionality of the population distributions. Furthermore, we will use the estimation of the Hellinger Distance from sample data as the target problem throughout this analysis so that we can compare estimation results between distributions of different configurations. For the rest of this section, we will only focus on the estimation from datasets with a Hellinger Distance of 0.5. We believe this slice of the results is sufficient in conveying the relevant characteristics of DeMoDivEst's scalability with respect to the number of binary variables.

From Figure 5a, we can observe that in general the raw difference between the estimated and actual Hellinger Distance increases monotonically as the number of binary

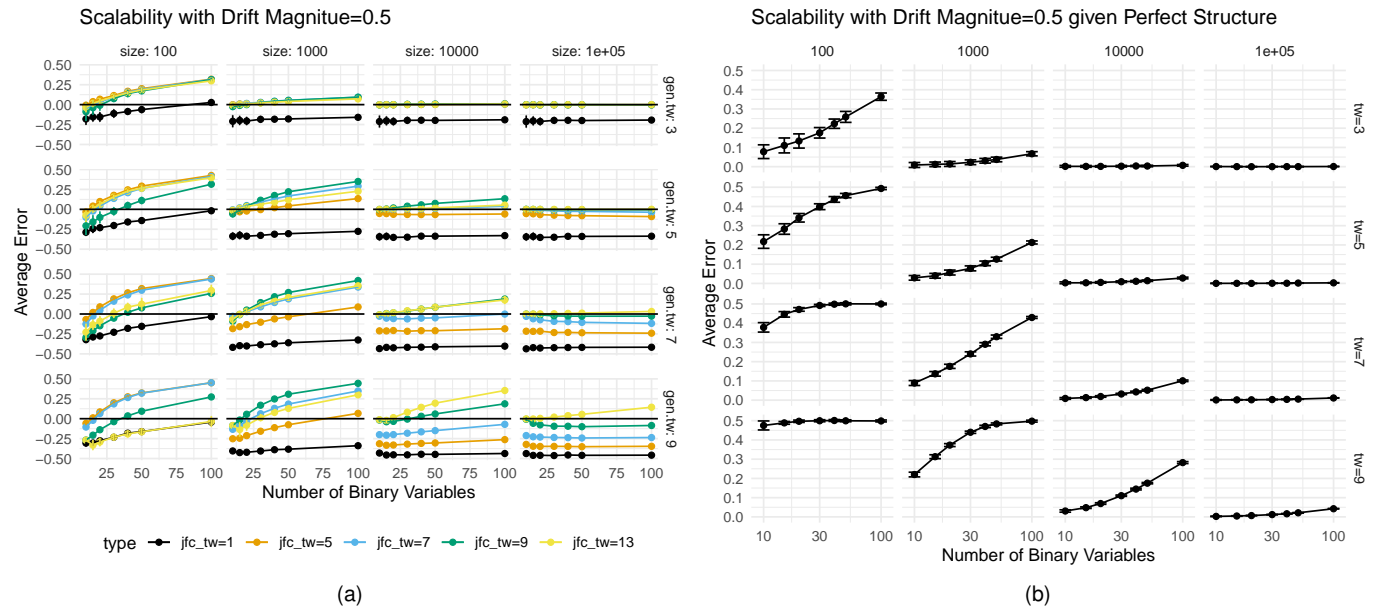


Fig. 5. Scalability of DeMoDivEst (w.r.t number of binary variables) at estimating the Hellinger Distance from sample data. Each row represents different treewidths for DeMoGen, each column represents the different sample sizes used for each of the 2 distributions. The x-axes represent the number of binary variables, the y-axes represent the raw difference between the estimated and actual Hellinger distance. Each point is the mean over the 50 different datasets with error bars representing the standard deviation. (a) contains results when a decomposable model is learnt from data while (b) contains results when the decomposable models used in DeMoGen are directly given to DeMoDivEst

variables increases. Furthermore, for DeMoGen treewidths of 3 and 5, the raw error is higher for DeMoDivEst with higher treewidths compared to DeMoDivEst with lower treewidths. However, for DeMoGen treewidths of 7 and 9, this is not necessarily the case. We can observe that for sample sizes of 100 and 1000, $jfc_tw=13$ is not necessarily the method with the highest raw error, in fact for a sample size of 100, both $jfc_tw=5$ and $jfc_tw=7$ have higher raw errors than $jfc_tw=9$ and $jfc_tw=13$.

However, an increase in raw error does not imply a decrease in estimation accuracy. In fact, in Figure 5a we can observe that an increase in raw error can result in an initial increase and later decrease in accuracy as the number of variables increases, or just a plain increase or decrease in accuracy. However, there are 2 things we can observe from Figure 5a. The first observation is that the initial estimate for most treewidth limits of DeMoDivEst underestimates the true Hellinger Distance when the number of variables is small. The second observation is that the estimated Hellinger Distance tend to increase as the number of variables increases, regardless of the initial estimate on low number of variables. Therefore, we hypothesise the following:

Hypothesis 1. the final error we observe is comprised 2 different types of errors:

- 1) errors due to inaccuracies in learning the structure of the decomposable model (structure error)
- 2) errors due to inaccuracies in parameter estimation (parameter estimation error)

In order to verify Hypothesis 1 and understand how both these types of errors affect the divergence estimation error, we ran an experiment to study the effects of just the parameter estimation error on the divergence estimation error.

This experiment is carried out by using the decomposable models created during the data generation process as the decomposable models of DeMoDivEst when estimating the Hellinger Distance from sample data. This eliminates any need to learn the structure of the decomposable model from sample data and thereby prevents structure error from occurring.

We can then use the results of this experiment to indirectly infer the effect structure error has on the divergence estimation error. We will not be studying the effect of structure error directly as it is hard to produce structure error without also producing parameter estimation error indirectly as well. Therefore, it is hard devising of an experiments which just studies the effect of only structure error.

From Figure 5b, the first thing we can observe is that the mean raw error decreases as we go from the leftmost column in the grid to the rightmost column. This is plainly just due to an increasing number of samples given to DeMoDivEst to estimate the Hellinger Distance. Furthermore, we can also observe that as the number of variables in the source distribution increases, the mean error increases as well. This is likely due to parameter estimation errors over each maximal clique propagating and accumulating throughout the entire model. As the number of variables increases, so does the number of maximal cliques within the decomposable model. Therefore, even if the parameter estimation error within any maximal clique of the same size is similar, the total parameter estimation error across the entire model will increase.

More importantly, we can observe from Figure 5b that if the structure of the decomposable models learnt by DeMoDivEst from data is perfect, DeMoDivEst consistently overestimates the true Hellinger Distance in the dataset. From this observation, we propose the following hypothesis:

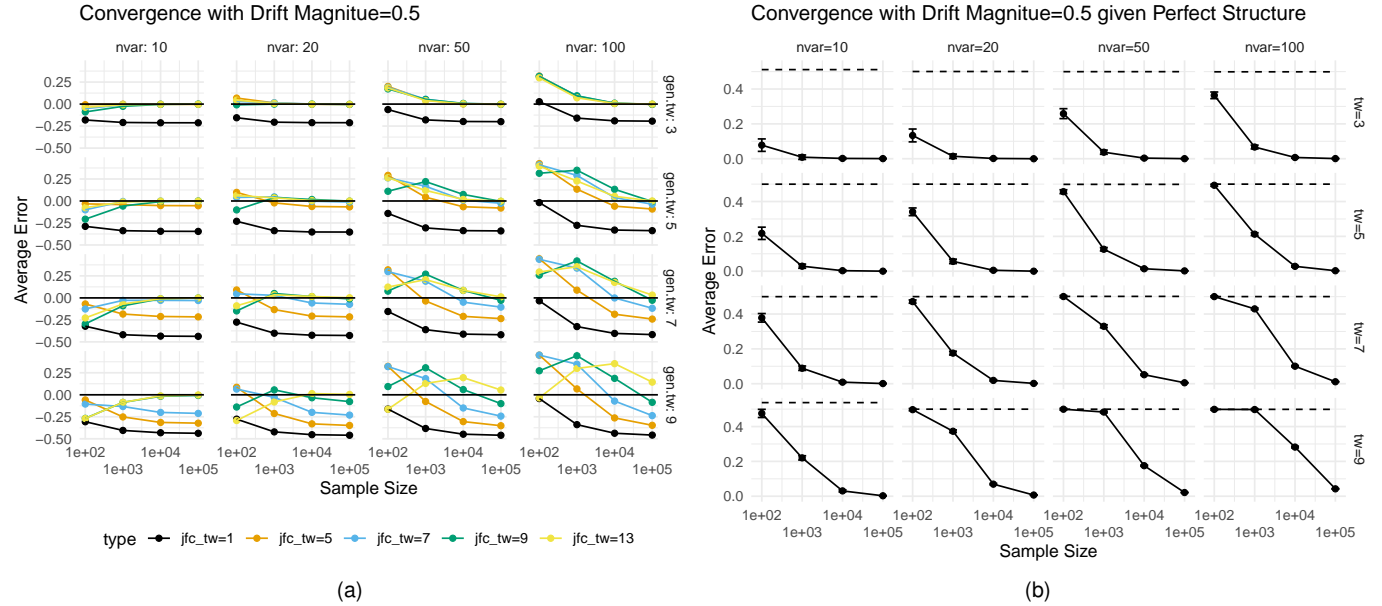


Fig. 6. Convergence of DeMoDivEst at estimating Hellinger Distance. Each row represents different generator treewidths, each column represents the different number of binary variables. The y-axes represent the raw difference between the estimated and actual Hellinger distance, the x-axes represent different sample sizes taken from the start of the first and second half of the generated data. Each point is the mean over the 50 different datasets generated with error bars representing the standard deviation. (a) contains results when the decomposable model is learnt from data while (b) contains results when the decomposable models used in DeMoGen are directly given to DeMoDivEst

Hypothesis 2. Assume we have 2 distributions, p and q , represented by 2 Decomposable Models, $\mathcal{M}_P = (G_p, \pi_p)$ and $\mathcal{M}_Q = (G_q, \pi_q)$, and 2 datasets, D_p and D_q , sampled from p and q respectively.

Let \hat{p} and \hat{q} be the estimates of the distributions p and q respectively. Both \hat{p} and \hat{q} are obtained using decomposable models, $\mathcal{M}_{\hat{p}} = (G_p, \hat{\pi}_p)$ and $\mathcal{M}_{\hat{q}} = (G_q, \hat{\pi}_q)$, learnt on the datasets D_p and D_q . Specifically, we fix the graph structure of both $\mathcal{M}_{\hat{p}}$ and $\mathcal{M}_{\hat{q}}$ to be the graph structure of the decomposable models representing the population distributions, G_p and G_q . The parameters, $\hat{\pi}_p$ and $\hat{\pi}_q$, are then learnt from the datasets D_p and D_q by learning the MLE of the multinomial distributions over each maximal clique and minimal separator of the graphs G_p and G_q . Given this setup, we then hypothesise that the expected Hellinger distance between the estimates \hat{p} and \hat{q} over multiple realisations of D_p and D_q will be greater than the actual Hellinger Distance between the true distributions p and q , or in other words:

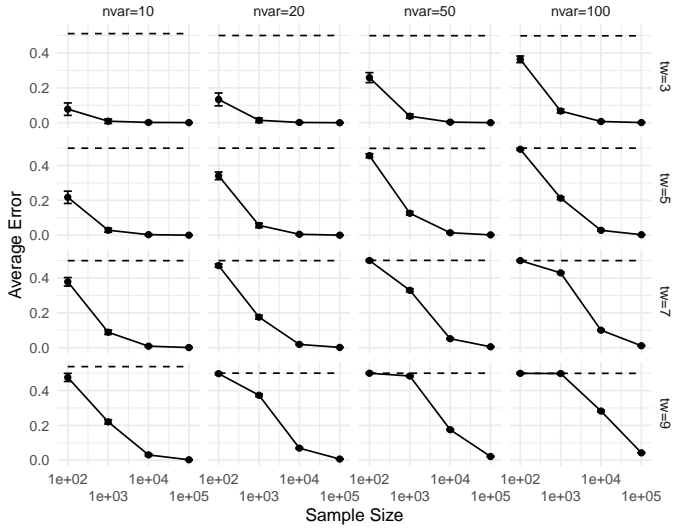
$$\mathbb{E}_{D_p, D_q} [H(\hat{p}, \hat{q})] > H(p, q)$$

Unfortunately, we do not have a formal proof for 2, however given the observations from Figure 5a, it seems likely that this is true.

Assuming Hypothesis 2 is true, we then propose the following hypothesis to explain the underestimation occurring in Figure 5a:

Hypothesis 3. Errors caused by learning an incorrect structure for the decomposable models used by DeMoDivEst will, on average, cause DeMoDivEst to underestimate the true Hellinger Distance, assuming sufficient data is provided to minimize parameter estimation error.

Convergence with Drift Magnitude=0.5 given Perfect Structure



We can use both Hypothesis 2 and 3 to help explain some of the behaviour exhibited by DeMoDivEst in Figure 5a. Specifically, from the first column of Figure 5a, representing results using just 100 data points from each population distribution, we can observe that $jfc_tw=13$ increasingly underestimates the Hellinger distance as the treewidth given to DeMoGen increases. If Hypothesis 3 is true, then this increase in underestimation for $jfc_tw=13$ should be due to increasing errors in the graph structure learnt by DeMoDivEst as DeMoGen's treewidth increases. Strangely enough, even though $jfc_tw=13$ is the method with the least restriction on its treewidth, it seems to have the greatest error caused by learning an incorrect graph structure when the sample size is low and the DeMoGen treewidth is high. This seems to imply that learning an incorrect model can cause a greater amount of divergence estimation error than to assume a greater amount of independence between the variables being modelled.

Furthermore, we can also observe a jump in overestimation for $jfc_tw=13$ from sample size 100 to sample size 1000 when DeMoGen has a treewidth of 9. This will be easier to observe if we rearrange the axes of the plots in Figure 5 such that the x axis of the plots represent the sample size used rather than the number of variables in the population distributions resulting in Figure 6a.

From Figure 6b we can see that, assuming DeMoDivEst has the same graph structure as the source distributions, DeMoDivEst will converge to the true Hellinger Distance as the number of samples increases. This result should not be too surprising as when the sample size increases, the estimated parameters in the decomposable models approaches the true parameters, and therefore the decomposable models in DeMoDivEst approaches the population distributions.

With this fact in mind, the plot in Figure 6a can seem

pretty counter-intuitive. Specifically, we can observe that for datasets with a high number of variables and a high treewidth for DeMoGen, the divergence estimation error of $jfc_{tw=13}$ increases as the sample size increases and then later decreases back down again after a certain point. We can also observe the same phenomena occurring for $jfc_{tw=9}$. We hypothesise that the cause of this phenomena is due to the reduction of structure error as the sample size available to DeMoDivEst increases. Furthermore, we hypothesise that this reduction in structure error, which according to Hypothesis 3 causes underestimation, reduces at a greater rate than the parameter estimation error, which according to Hypothesis 2 causes overestimation. This gives the illusion that the divergence estimation error increases as the sample size increases, when really, we believe it is caused by the reduction of structure error, revealing the true error caused by parameter estimation.

8 CONCLUSION

In conclusion, we showed that it is possible to use decomposable models to leverage possible structures between variables in order to assist with estimating the divergence between 2 high-dimensional distributions using sample data. The advantage of leveraging the variable structure is that it allows our divergence estimation approach, DeMoDivEst, to scale with respect to the treewidth of the decomposable models learnt from the data. Furthermore, leveraging the variable structure helps prevent the complexity of DeMoDivEst from increasing exponentially with respect to the number of variables provided that the distributions of interest do not have a fully saturated variable structure.

The work presented represents a proof of concept that decomposable models can indeed assist in the problem of divergence estimation. Therefore, there are many possible avenues of further research that can be carried out to extend the work presented here. For instance, in this paper, we used the empirical distribution to estimate the clique probabilities in the decomposable models learnt from the data. However, it is possible to use more statistically efficient estimators for clique probability estimation, such as the Profile Maximum Likelihood mentioned in Section 6, and more work is needed to find, adapt, and test existing estimators on this approach of divergence estimation. Furthermore, throughout his work, we only considered estimating the divergence between 2 discrete distributions. Therefore, more work is needed to investigate how one might extend this approach for divergence estimation to numeric or even mixed type data. Additionally, when obtaining the computation graph in conjunction with the decomposable models from the available samples, we assumed that variable structure of the 2 distributions are the same. However, this assumption does not necessarily hold in real data. Our methods are already capable of estimating diverges between distributions modelled by decomposable models with different structures, save for the missing link of a robust method for deriving useful computation graphs for such models. In consequence, more work is needed to develop more sophisticated techniques for obtaining the computation graph in conjunction with the decomposable models estimating the distributions of interest.

ACKNOWLEDGMENTS

This research has been supported by the Federal Ministry of Education and Research of Germany as part of the competence center for machine learning ML2R (01IS18038B) as well as the Fraunhofer Research Center Machine Learning, the Australian Research Council under award DP190100017, and an Australian Government Research Training Program (RTP) Scholarship.

REFERENCES

- [1] J. C. Schlimmer and R. H. Granger, "Incremental learning from noisy data," *Mach. Learn.*, vol. 1, no. 3, pp. 317–354, sep 1986.
- [2] G. I. Webb, R. Hyde, H. Cao, H. L. Nguyen, and F. Petitjean, "Characterizing concept drift," *Data Min. Knowl. Discov.*, vol. 30, no. 4, pp. 964–994, jul 2016.
- [3] G. I. Webb, L. K. Lee, B. Goethals, and F. Petitjean, "Analyzing concept drift and shift from sample data," *Data Min. Knowl. Discov.*, vol. 32, no. 5, pp. 1179–1199, sep 2018.
- [4] B. Barz, E. Rodner, Y. G. Garcia, and J. Denzler, "Detecting regions of maximal divergence for spatio-temporal anomaly detection," *IEEE Trans. Pattern Anal. Mach. Intell.*, vol. 41, no. 5, pp. 1088–1101, may 2019.
- [5] Y. Chen, J. Ye, and J. Li, "Aggregated Wasserstein Distance and State Registration for Hidden Markov Models," *IEEE Trans. Pattern Anal. Mach. Intell.*, vol. 42, no. 9, pp. 2133–2147, sep 2020.
- [6] J. M. Hammersley and P. Clifford, "Markov fields on finite graphs and lattices," *Unpublished manuscript*, 1971.
- [7] J. Besag, "Statistical analysis of non-lattice data," *Journal of the Royal Statistical Society. Series D (The Statistician)*, vol. 24, no. 3, pp. 179–195, 1975.
- [8] A. Cichocki, S. Cruces, and S.-i. Amari, "Generalized Alpha-Beta Divergences and Their Application to Robust Nonnegative Matrix Factorization," *Entropy*, vol. 13, no. 1, pp. 134–170, jan 2011.
- [9] A. W. van der Vaart, *Asymptotic Statistics*, ser. Cambridge Series in Statistical and Probabilistic Mathematics. Cambridge: Cambridge University Press, oct 1998.
- [10] F. Petitjean, G. I. Webb, and A. E. Nicholson, "Scaling Log-Linear Analysis to High-Dimensional Data," in *2013 IEEE 13th Int. Conf. Data Min.* Dallas, TX, USA: IEEE, dec 2013, pp. 597–606.
- [11] F. Petitjean, L. Allison, and G. I. Webb, "A Statistically Efficient and Scalable Method for Log-Linear Analysis of High-Dimensional Data," in *2014 IEEE Int. Conf. Data Min.*, vol. 2015-Janua, no. January. Shenzhen, China: IEEE, dec 2014, pp. 480–489.
- [12] F. Petitjean and G. I. Webb, "Scaling log-linear analysis to datasets with thousands of variables," in *Proc. 2015 SIAM Int. Conf. Data Min.* Philadelphia, PA: Society for Industrial and Applied Mathematics, jun 2015, pp. 469–477.
- [13] G. I. Webb and F. Petitjean, "A Multiple Test Correction for Streams and Cascades of Statistical Hypothesis Tests," in *Proc. 22nd ACM SIGKDD Int. Conf. Knowl. Discov. Data Min.*, vol. 13-17-Augu. New York, NY, USA: ACM, aug 2016, pp. 1255–1264.
- [14] M. J. Wainwright and M. I. Jordan, "Graphical models, exponential families, and variational inference," *Foundations and Trends in Machine Learning*, vol. 1, no. 1–2, pp. 1–305, 2008.
- [15] L. G. Valiant, "The complexity of enumeration and reliability problems," *SIAM Journal on Computing*, vol. 8, no. 3, pp. 410–421, 1979.
- [16] A. Bulatov and M. Grohe, "The complexity of partition functions," in *Automata, Languages and Programming*, ser. Lecture Notes in Computer Science. Heidelberg, Germany: Springer, 2004, vol. 3142, pp. 294–306.
- [17] D. V. Gokhale and S. J. Haberman, *The Analysis of Frequency Data*. University of Chicago Press, dec 1975, vol. 31, no. 4.
- [18] S. L. Lauritzen and D. J. Spiegelhalter, "Local computations with probabilities on graphical structures and their application to expert systems," *Journal of the Royal Statistical Society. Series B (Methodological)*, vol. 50, no. 2, pp. 157–224, 1988.
- [19] D. Koller and N. Friedman, *Probabilistic Graphical Models - Principles and Techniques*. MIT Press, 2009.
- [20] R. Dechter, *Constraint processing*. Elsevier Morgan Kaufmann, 2003.
- [21] A. Berry, S. J. R. Blair, P. Heggernes, and W. B. Peyton, "Maximum cardinality search for computing minimal triangulations of graphs," *Algorithmica*, vol. 39, no. 4, pp. 287–298, 2004.

- [22] P. Heggernes, "Minimal triangulations of graphs: A survey," *Discrete Mathematics*, vol. 306, no. 3, pp. 297–317, 2006.
- [23] J. Acharya, "Profile Maximum Likelihood is Optimal for Estimating KL Divergence," in *IEEE Int. Symp. Inf. Theory - Proc.*, vol. 2018-June, 2018, pp. 1400–1404.
- [24] D. S. Pavlichin, J. Jiao, and T. Weissman, "Approximate profile maximum likelihood," *J. Mach. Learn. Res.*, vol. 20, no. 122, pp. 1–55, 2019.
- [25] Z. Zhang and M. Grabchak, "Nonparametric Estimation of Kullback-Leibler Divergence," *Neural Comput.*, vol. 26, no. 11, pp. 2570–2593, nov 2014.
- [26] Y. Han, J. Jiao, and T. Weissman, "Minimax rate-optimal estimation of KL divergence between discrete distributions," in *Proc. 2016 Int. Symp. Inf. Theory Its Appl. ISITA 2016*, may 2017, pp. 256–260.
- [27] ———, "Minimax Estimation of Divergences Between Discrete Distributions," *IEEE J. Sel. Areas Inf. Theory*, vol. 1, no. 3, pp. 814–823, nov 2020.
- [28] Y. Bu, S. Zou, Y. Liang, and V. V. Veeravalli, "Estimation of KL Divergence: Optimal Minimax Rate," *IEEE Trans. Inf. Theory*, vol. 64, no. 4, pp. 2648–2674, apr 2018.
- [29] J. Jiao, Y. Han, and T. Weissman, "Minimax estimation of the L1 distance," *IEEE Trans. Inf. Theory*, vol. 64, no. 10, pp. 6672–6706, oct 2018.
- [30] A. Orlitsky, N. Santhanam, K. Viswanathan, and J. Zhang, "On Modeling Profiles instead of Values," in *Proc. 20th Conf. Uncertain. Artif. Intell.*, ser. UAI '04. Arlington, Virginia, USA: AUAI Press, jul 2014, pp. 426–435.

Loong Kuan Lee is currently a PhD candidate at Monash University, Melbourne, Australia. Lee's primary research area is concept drift in machine learning.

Nico Piatkowski received his B.Sc., Dipl.-Inf. and Dr. rer. nat. degrees from TU Dortmund University, Dortmund, Germany. He is currently a senior research scientist at the Media Engineering Group of the Fraunhofer Institute for Intelligent Analysis and Information Systems IAIS in Sankt Augustin, Germany. Before that, he was a research scientist at the Artificial Intelligence Unit at TU Dortmund, at the DFG Collaborative Research Center SFB 876 on "Providing Information by Resource-Constrained Data Analysis", and then the Competence Center Machine Learning Rhine-Ruhr (ML2R). Nico contributed to various research projects on the foundations of machine learning under resource constraints, spatio-temporal modelling, and probabilistic inference. His current research interest is focused on quantum computing methods for structural and probabilistic inference.

François Petitjean François Petitjean obtained his PhD in 2012 with the French Space Agency on the automatic analysis of satellite images, PhD for which he received multiple awards. He has published 50+ scientific articles in leading journals and conferences in Data Science and Machine Learning. His current research interests revolve around Data Science for Social and Environmental Good.

Geoff Webb received his B.A. and PhD degrees from La Trobe University, Australia. He is currently a Professor in the Department of Data Science and Artificial Intelligence and Research Director of the Monash Data Futures Institute at Monash University, Australia. Geoff's primary research areas are machine learning, data mining and computational structural biology. He was editor-in-chief of Data Mining and Knowledge Discovery from 2005 to 2014. He is an IEEE Fellow and his many awards include the 2013 IEEE ICDM Service Award and the inaugural Eureka Prize for Excellence in Data Science (2017).

APPENDIX A

PROOF OF THEOREM 1

When $\alpha, \beta, \alpha + \beta \neq 0$:

$$\begin{aligned} D_{AB}^{\alpha, \beta}(\mathbb{P}, \mathbb{Q}) &= -\frac{1}{\alpha\beta} \left(\sum_{\hat{x}} \mathbb{P}(\hat{x})^\alpha \mathbb{Q}(\hat{x})^\beta - \frac{\alpha}{\alpha + \beta} \sum_{\hat{x}} \mathbb{P}(\hat{x})^{\alpha+\beta} - \frac{\beta}{\alpha + \beta} \sum_{\hat{x}} \mathbb{Q}(\hat{x})^{\alpha+\beta} \right) \\ &= -\frac{1}{\alpha\beta} \left(f_1(\mathbb{P}, \mathbb{Q}; \alpha, \beta) - \frac{\alpha}{\alpha + \beta} f_1(\mathbb{P}, \mathbb{Q}; \alpha + \beta, 0) - \frac{\beta}{\alpha + \beta} f_1(\mathbb{P}, \mathbb{Q}; 0, \alpha + \beta) \right) \end{aligned}$$

When $\alpha \neq 0, \beta = 0$:

$$\begin{aligned} D_{AB}^{\alpha, \beta}(\mathbb{P} || \mathbb{Q}) &= \frac{1}{\alpha^2} \left(\sum_{\hat{x}} \mathbb{P}(\hat{x})^\alpha \ln \frac{\mathbb{P}(\hat{x})^\alpha}{\mathbb{Q}(\hat{x})^\alpha} - \sum_{\hat{x}} \mathbb{P}(\hat{x})^\alpha + \sum_{\hat{x}} \mathbb{Q}(\hat{x})^\alpha \right) \\ &= \frac{1}{\alpha^2} (f_2(\mathbb{P}, \mathbb{Q}; \alpha, 0, \alpha, -\alpha) - f_1(\mathbb{P}, \mathbb{Q}; \alpha, 0) + f_1(\mathbb{P}, \mathbb{Q}; 0, \alpha)) \end{aligned}$$

When $\alpha = -\beta \neq 0$:

$$\begin{aligned} D_{AB}^{\alpha, \beta}(\mathbb{P} || \mathbb{Q}) &= \frac{1}{\beta^2} \left(\sum_{\hat{x}} \mathbb{Q}(\hat{x})^\beta \ln \frac{\mathbb{Q}(\hat{x})^\beta}{\mathbb{P}(\hat{x})^\beta} - \sum_{\hat{x}} \mathbb{Q}(\hat{x})^\beta + \sum_{\hat{x}} \mathbb{P}(\hat{x})^\beta \right) \\ &= \frac{1}{\beta^2} (f_2(\mathbb{P}, \mathbb{Q}; 0, \beta, -\beta, \beta) - f_1(\mathbb{P}, \mathbb{Q}; 0, \beta) + f_1(\mathbb{P}, \mathbb{Q}; \beta, 0)) \end{aligned}$$

When $\alpha = 0, \beta \neq 0$:

$$\begin{aligned} D_{AB}^{\alpha, \beta}(\mathbb{P} || \mathbb{Q}) &= \frac{1}{2} \left(\sum_{\hat{x}} \ln \mathbb{P}(\hat{x}) - \sum_{\hat{x}} \ln \mathbb{Q}(\hat{x}) \right)^2 \\ &= f_3(\mathbb{P}, \mathbb{Q}) \end{aligned}$$

When $\alpha, \beta = 0$:

$$\begin{aligned} D_{AB}^{\alpha, \beta}(\mathbb{P} || \mathbb{Q}) &= \frac{1}{2} \left(\sum_{\hat{x}} \ln \mathbb{P}(\hat{x}) - \sum_{\hat{x}} \ln \mathbb{Q}(\hat{x}) \right)^2 \\ &= f_3(\mathbb{P}, \mathbb{Q}) \end{aligned}$$

□

APPENDIX B

PROOF OF THEOREM 2

Recall the $\alpha\beta$ -divergence when $\alpha, \beta = 0$:

$$\begin{aligned} D_{AB}^{\alpha, \beta}(\mathbb{P} || \mathbb{Q}) &= \frac{1}{2} \left(\sum_{\hat{x} \in \mathcal{X}} \ln \mathbb{P}(\hat{x}) - \sum_{\hat{x}} \ln \mathbb{Q}(\hat{x}) \right)^2 \\ &= \frac{1}{2} \left(\sum_{\hat{x} \in \mathcal{X}} \ln \prod_{C \in \mathcal{C}_{\mathbb{P}}} \mathbb{P}_{\text{CPT}(C)}(\hat{x}) - \sum_{\hat{x} \in \mathcal{X}} \ln \prod_{C \in \mathcal{C}_{\mathbb{Q}}} \mathbb{Q}_{\text{CPT}(C)}(\hat{x}) \right) \\ &= \frac{1}{2} \left(\sum_{\hat{x} \in \mathcal{X}} \sum_{C \in \mathcal{C}_{\mathbb{P}}} \ln \mathbb{P}_{\text{CPT}(C)}(\hat{x}) - \sum_{\hat{x} \in \mathcal{X}} \sum_{C \in \mathcal{C}_{\mathbb{Q}}} \ln \mathbb{Q}_{\text{CPT}(C)}(\hat{x}) \right) \\ &= \frac{1}{2} \left(\sum_{C \in \mathcal{C}_{\mathbb{P}}} \sum_{\hat{x} \in \mathcal{X}_C} \ln \mathbb{P}_{\text{CPT}(C)}(\hat{x}) - \sum_{C \in \mathcal{C}_{\mathbb{Q}}} \sum_{\hat{x} \in \mathcal{X}_C} \ln \mathbb{Q}_{\text{CPT}(C)}(\hat{x}) \right) \end{aligned} \tag{9}$$

We can find the complexity of solely computing the sums in Equation 9, without considering the complexity of obtaining the terms in the sums, by computing the following:

$$\begin{aligned} \sum_{C \in \mathcal{C}_{\mathbb{P}}} \sum_{\hat{x} \in \mathcal{X}_C} 1 + \sum_{C \in \mathcal{C}_{\mathbb{Q}}} \sum_{\hat{x} \in \mathcal{X}_C} 1 &\in \sum_{C \in \mathcal{C}_{\mathbb{P}}} \mathcal{O}(2^{|C|}) + \sum_{C \in \mathcal{C}_{\mathbb{Q}}} \mathcal{O}(2^{|C|}) \\ &\in \mathcal{O}(|\mathcal{C}(\mathcal{G}_{\mathbb{P}})|2^{tw(\mathcal{G}_{\mathbb{P}})}) + \mathcal{O}(|\mathcal{C}(\mathcal{G}_{\mathbb{Q}})|2^{tw(\mathcal{G}_{\mathbb{Q}})}) \end{aligned}$$

where

$$tw(\mathcal{G}) = \max\{|C| : C \in \mathcal{C}(\mathcal{G}_{\mathbb{P}})\}$$

This holds as the treewidth of a graph \mathcal{G} , $tw(\mathcal{G})$, is the size of the largest maximal clique in \mathcal{G} and therefore is an upper bound on the size of all the maximal cliques in \mathcal{G} . \square

APPENDIX C

PROOF OF THEOREM 3

Recall \mathcal{F} :

$$\mathcal{F}(\mathbb{P}, \mathbb{Q}) = \sum_{\hat{x} \in \mathcal{X}} g[\mathbb{P}(\hat{x})] \cdot h[\mathbb{Q}(\hat{x})] \cdot L(g^*[\mathbb{P}(\hat{x})] \cdot h^*[\mathbb{Q}(\hat{x})])^l$$

Then recall f_1 from Theorem 1:

$$f_1(\mathbb{P}, \mathbb{Q}; a, b) = \sum_{\hat{x}} \mathbb{P}(\hat{x})^a \mathbb{Q}(\hat{x})^b$$

therefore, $f_1(\mathbb{P}, \mathbb{Q}; a, b) = \mathcal{F}(\mathbb{P}, \mathbb{Q})$ when

$$\begin{aligned} h(x) &= x^a & g(x) &= x^b \\ l &= 0 \Rightarrow L, g^*, h^* \text{ are irrelevant} \end{aligned}$$

Also recall f_2 from Theorem 1:

$$f_2(\mathbb{P}, \mathbb{Q}; a, b, c, d) = \sum_{\hat{x}} \mathbb{P}(\hat{x})^a \mathbb{Q}(\hat{x})^b \ln \left(\mathbb{P}(\hat{x})^c \mathbb{Q}(\hat{x})^d \right)$$

therefore, $f_2(\mathbb{P}, \mathbb{Q}; a, b, c, d) = \mathcal{F}(\mathbb{P}, \mathbb{Q})$ when

$$\begin{aligned} h(x) &= x^a & h^*(x) &= x^c \\ g(x) &= x^b & g^*(x) &= x^d \\ l &= 1 & L(x) &= \ln x \end{aligned}$$

\square

APPENDIX D

PROOF OF REMARK 1

The lower bound complexity can be computed by multiplying the cardinality of each sum in the 2 nested sum of Equation 4 to get $(|\mathcal{C}(\mathcal{G}_{\mathbb{P}})| + |\mathcal{C}(\mathcal{G}_{\mathbb{Q}})|) |\mathcal{X}|$. Since the lower bound of the number of cliques in $\mathcal{G}_{\mathbb{P}}$ and $\mathcal{G}_{\mathbb{Q}}$ is 1, therefore the expression is in $\Omega(2^{|\mathcal{X}|})$. The last expression is in Therefore, the lower bound complexity of naively computing Equation 4 is exponential with respect to the number of variables in decomposable models $\mathcal{M}_{\mathbb{P}}$ and $\mathcal{M}_{\mathbb{Q}}$. \square

APPENDIX E

PROOF OF THEOREM 4

We first show that the equivalence in Equation 6 holds. This will then imply that the equivalence in Equation 7 holds as well since the exact same steps can be used for showing this equivalence holds as well.

Starting from the left hand side of Equation 6, we can split the innermost sum into 2 sums, one over the set $\mathcal{X}_{\alpha(C)-C}$ and $\mathcal{X}_{X-\alpha(C)}$, then move the sum over $\mathcal{X}_{\alpha(C)-C}$ outside and merge it with the sum over \mathcal{X}_C :

$$\begin{aligned} & \sum_{C \in \mathcal{C}_{\mathbb{P}}} \sum_{\hat{x}_C \in \mathcal{X}_C} L \left(g^* \left[\hat{\mathbb{P}}_C^{\text{JT}}(\hat{x}_C) \right] \right)^l S P_C(\hat{x}_C) \\ &= \sum_{C \in \mathcal{C}_{\mathbb{P}}} \sum_{\hat{x}_C \in \mathcal{X}_C} L \left(g^* \left[\hat{\mathbb{P}}_C^{\text{JT}}(\hat{x}_C) \right] \right)^l \sum_{\hat{x} \in \mathcal{X}_{X-\alpha(C)}} g \left[\hat{\mathbb{P}}(\hat{x}_C, \hat{x}) \right] h \left[\hat{\mathbb{Q}}(\hat{x}_C, \hat{x}) \right] \\ &= \sum_{C \in \mathcal{C}_{\mathbb{P}}} \sum_{\hat{x}_C \in \mathcal{X}_C} L \left(g^* \left[\hat{\mathbb{P}}_C^{\text{JT}}(\hat{x}_C) \right] \right)^l \sum_{\hat{x} \in \mathcal{X}_{X-\alpha(C)+\alpha(C)-C}} g \left[\hat{\mathbb{P}}(\hat{x}_C, \hat{x}) \right] h \left[\hat{\mathbb{Q}}(\hat{x}_C, \hat{x}) \right] \\ &= \sum_{C \in \mathcal{C}_{\mathbb{P}}} \sum_{\hat{x}_C \in \mathcal{X}_C} \sum_{\hat{x}' \in \mathcal{X}_{\alpha(C)-C}} L \left(g^* \left[\hat{\mathbb{P}}_C^{\text{JT}}(\hat{x}_C, \hat{x}') \right] \right)^l \sum_{\hat{x} \in \mathcal{X}_{X-\alpha(C)}} g \left[\hat{\mathbb{P}}(\hat{x}_C, \hat{x}, \hat{x}') \right] h \left[\hat{\mathbb{Q}}(\hat{x}_C, \hat{x}, \hat{x}') \right] \\ &= \sum_{C \in \mathcal{C}_{\mathbb{P}}} \sum_{\hat{x}_{\alpha(C)} \in \mathcal{X}_{\alpha(C)}} L \left(g^* \left[\hat{\mathbb{P}}_C^{\text{JT}}(\hat{x}_{\alpha(C)}) \right] \right)^l \sum_{\hat{x} \in \mathcal{X}_{X-\alpha(C)}} g \left[\hat{\mathbb{P}}(\hat{x}_{\alpha(C)}, \hat{x}) \right] h \left[\hat{\mathbb{Q}}(\hat{x}_{\alpha(C)}, \hat{x}) \right] \\ &= \sum_{C \in \mathcal{C}_{\mathbb{P}}} \sum_{\hat{x}_{\alpha(C)} \in \mathcal{X}_{\alpha(C)}} L \left(g^* \left[\hat{\mathbb{P}}_C^{\text{JT}}(\hat{x}_{\alpha(C)}) \right] \right)^l S P_{\alpha(C)}(\hat{x}_{\alpha(C)}) \end{aligned}$$

□

APPENDIX F

PROOF OF THEOREM 5

Since, by Definition 4, there exist a mapping, α , from the maximal cliques in $\mathcal{M}_{\mathbb{P}}$ and $\mathcal{M}_{\mathbb{Q}}$ to a maximal clique in the computation graph \mathcal{H} . Therefore, each element in the factor set Φ can be mapped to a maximal clique in \mathcal{H} as well.

The existence of this mapping allows us to run a junction tree algorithm over the junction tree of graph \mathcal{H} , $\mathcal{T} = (\mathcal{C}, \mathcal{S})$, using Φ as factors.

Recall from Section 2.2 that given a chordal graph \mathcal{H} and a set of factors $\Phi = \{\phi_i\}$, the Junctions Tree Algorithm provides the following belief for each maximal clique in the Junction Tree, $\mathcal{T} = (\mathcal{C}, \mathcal{S})$, of the chordal graph \mathcal{H} :

$$\forall C \in \mathcal{C} : \beta_C(\hat{x}_C) = \sum_{\hat{x} \in \mathcal{X}_{\hat{X}-C}} \prod_{\phi \in \Phi} \phi(\hat{x}, \hat{x}_C)$$

By using the set of factors Φ defined in Theorem 5, we directly obtain the following by simple substitution:

$$\forall C \in \mathcal{C} :$$

$$\begin{aligned} \beta_C(\hat{x}_C) &= \sum_{\hat{x} \in \mathcal{X}_{\hat{X}-C}} \prod_{C_{\mathbb{P}} \in \mathcal{C}(\mathcal{G}_{\mathbb{P}})} g\left[\hat{\mathbb{P}}_{C_{\mathbb{P}}}^{\text{JT}}(\hat{x}, \hat{x}_C)\right] \prod_{C_{\mathbb{Q}} \in \mathcal{C}(\mathcal{G}_{\mathbb{Q}})} h\left[\hat{\mathbb{Q}}_{C_{\mathbb{Q}}}^{\text{JT}}(\hat{x}, \hat{x}_C)\right] \\ &= SP_C(\hat{x}_C) \end{aligned}$$

□

APPENDIX G

PROOF OF COROLLARY 1

As we have showed in Section 4.1, computing $\mathcal{F}(\mathbb{P}, \hat{\mathbb{Q}})$ involves 3 steps:

- 1) Running the junction tree algorithm once to obtain the beliefs over each maximal clique in \mathcal{H} with factors from $g\left[\hat{\mathbb{P}}(\hat{x})\right]$ and $h\left[\hat{\mathbb{Q}}(\hat{x})\right]$. The time complexity for this step is bounded by an exponential with respect to the treewidth of \mathcal{H} .
- 2) Multiplying each belief by an additional term, $L(\cdot)$, summing over the belief by its domain. This step is also bounded by an exponential with respect to the treewidth of \mathcal{H} .
- 3) Repeating the previous step for each maximal clique in decomposable models $\mathcal{M}_{\mathbb{P}}$ and $\mathcal{M}_{\mathbb{Q}}$. This results in multiplying the complexity of the previous step by the number of maximal cliques in $\mathcal{M}_{\mathbb{P}}$ and $\mathcal{M}_{\mathbb{Q}}$, $|\mathcal{C}(\mathcal{G}_{\mathbb{P}})|$ and $|\mathcal{C}(\mathcal{G}_{\mathbb{Q}})|$ respectively.

Therefore the resulting complexity is:

$$\begin{aligned} &(|\mathcal{C}(\mathcal{G}_{\mathbb{P}})| + |\mathcal{C}(\mathcal{G}_{\mathbb{Q}})|) \cdot \mathcal{O}\left(2^{\text{tw}(\mathcal{H})}\right) + \mathcal{O}\left(2^{\text{tw}(\mathcal{H})}\right) \\ &= \mathcal{O}\left(|\mathcal{C}(\mathcal{G}_{\mathbb{P}})| + |\mathcal{C}(\mathcal{G}_{\mathbb{Q}})| \cdot 2^{\text{tw}(\mathcal{H})}\right) \end{aligned}$$

□

APPENDIX H

PROOF OF THEOREM 6

Recall from Equation 5, $\forall C \in \mathcal{C}(\mathcal{G}_{\mathbb{P}}, \mathcal{G}_{\mathbb{Q}})$:

$$SP_{\alpha(C)}(\hat{x}_{\alpha(C)}) = \sum_{\hat{x} \in \mathcal{X}_{\hat{X}-\alpha(C)}} \left[\prod_{C_{\mathbb{P}} \in \mathcal{C}_{\mathbb{P}}} g\left[\hat{\mathbb{P}}_{C_{\mathbb{P}}}^{\text{JT}}(\hat{x}_{\alpha(C)}, \hat{x})\right] \right] \left[\prod_{C_{\mathbb{Q}} \in \mathcal{C}_{\mathbb{Q}}} h\left[\hat{\mathbb{Q}}_{C_{\mathbb{Q}}}^{\text{JT}}(\hat{x}_{\alpha(C)}, \hat{x})\right] \right]$$

Following the usual steps to initiate the junction tree algorithm, we define the set of factors, Φ , to use in the junction tree algorithm as such:

$$\Phi = \left\{ g\left(\hat{\mathbb{P}}_C^{\text{JT}}\right) : C \in \mathcal{C}_{\mathbb{P}} \right\} \cup \left\{ h\left(\hat{\mathbb{Q}}_C^{\text{JT}}\right) : C \in \mathcal{C}_{\mathbb{Q}} \right\}$$

As usual at the start of the junction tree algorithm, each factor in Φ is assigned to a maximal clique in the junction tree, or in this case junction forest, of the computation graph \mathcal{H} . These assignments will use the clique mapping function from Definition 4, α , and the factors assigned into each maximal clique in \mathcal{G} are multiplied together into the initial belief for each clique ψ_i :

$$\forall C \in \mathcal{C}(\mathcal{H}) : \psi_C = \prod_{C_{\mathbb{P}} \in A_C(\mathcal{C}(\mathcal{G}_{\mathbb{P}}))} g\left(\hat{\mathbb{P}}_{C_{\mathbb{P}}}^{\text{JT}}\right) \prod_{C_{\mathbb{Q}} \in A_C(\mathcal{C}(\mathcal{G}_{\mathbb{Q}}))} h\left(\hat{\mathbb{Q}}_{C_{\mathbb{Q}}}^{\text{JT}}\right)$$

Then SP can be re-expressed in terms of these initial clique beliefs ψ :

$$SP_{\alpha(C)}(\hat{x}_{\alpha(C)}) = \sum_{\hat{x} \in \mathcal{X}_{\hat{X} - \alpha(C)}} \prod_{C_{\mathcal{H}} \in \mathcal{C}(\mathcal{H})} \psi_{C_{\mathcal{H}}}(\hat{x}_{\alpha(C)}, \hat{x})$$

Due to the independence between maximal cliques of different junction trees in the junction forest \mathcal{T} , we can split the sum in SP into a product of sum-products over each junction tree in \mathcal{T} :

$$\begin{aligned} SP_{\alpha(C)}(\hat{x}_{\alpha(C)}) &= \sum_{\hat{x} \in \mathcal{X}_{\hat{X} - \alpha(C)}} \prod_{C_{\mathcal{H}} \in \mathcal{C}(\mathcal{H})} \psi_{C_{\mathcal{H}}}(\hat{x}_{\alpha(C)}, \hat{x}) \\ &= \sum_{\hat{x} \in \mathcal{X}_{\hat{X} - \alpha(C)}} \prod_{T \in \mathcal{T}} \prod_{C_{\mathcal{H}} \in \mathcal{C}(T)} \psi_{C_{\mathcal{H}}}(\hat{x}_{\alpha(C)}, \hat{x}) \\ &= \sum_{\hat{x}_{T_1} \in \mathcal{X}_{\mathcal{C}(T_1)}} \cdots \sum_{\hat{x}_{\tau(C)} \in \mathcal{X}_{\mathcal{C}(\tau(C)) - \alpha(C)}} \cdots \sum_{\hat{x}_{T_{|\mathcal{T}|}} \in \mathcal{X}_{\mathcal{C}(T_{|\mathcal{T}|})}} \prod_{T \in \mathcal{T}} \prod_{C_{\mathcal{H}} \in \mathcal{C}(T)} \psi_{C_{\mathcal{H}}}(\hat{x}_{T_1}, \dots, \hat{x}_{\tau(c)}, \dots, \hat{x}_{T_{|\mathcal{T}|}}) \\ &= \left(\sum_{\hat{x}_{\tau(C)} \in \mathcal{X}_{\mathcal{C}(\tau(C)) - \alpha(C)}} \prod_{C_{\mathcal{H}} \in \mathcal{C}(\tau(C))} \psi_{C_{\mathcal{H}}}(\hat{x}_{\tau(C)}) \right) \prod_{T \in \mathcal{T} - \tau(C)} \left(\sum_{\hat{x}_T \in \mathcal{X}_{\mathcal{C}(T)}} \prod_{C_{\mathcal{H}} \in \mathcal{C}(T)} \psi_{C_{\mathcal{H}}}(\hat{x}_T) \right) \\ &= \beta_{\alpha(C)}(\hat{x}_{\alpha(C)}) \prod_{T \in \mathcal{T} - \tau(C)} \sum_{\hat{x} \in \mathcal{X}_{\mathcal{C}(T)}} \beta_{C(T)}(\hat{x}_{\alpha(C)}, \hat{x}) \end{aligned}$$

□